SEMMELWEIS EGYETEM
DOKTORI ISKOLA

Ph.D. értekezések

3106.

ISTVÁN LILLA

Szemészet
című program

Programvezető: Dr. Nagy Zoltán Zsolt, egyetemi tanár
Témavezető: Dr. Kovács Illés, egyetemi docens

MEASUREMENT OF THE RETINAL MICROVASCULAR BLOOD FLOW BY OCT ANGIOGRAPHY TO ASSESS RISK FACTORS AND POSTOPERATIVE PERFUSION IMPROVEMENT IN PATIENTS WITH CAROTID ARTERY STENOSIS

Ph.D. thesis

Lilla István

Surgical Medicine Division
Doctoral College, Semmelweis University

Supervisor: Illés Kovács, MD, Ph.D.

Official reviewers: Mária Éva Ferencz, MD, Ph.D.
Kinga Kránitz, MD, Ph.D.

Complex Examination Committee:
Head: László Harsányi, MD, Ph.D.
Members: Mária Éva Ferencz, MD, Ph.D.
Antal Szabó, MD, Ph.D.

Budapest
2024

Table of contents

List of Abbreviations

ACA: anterior cerebral artery

ACoA: anterior communicating artery

AMD: age-related macular degeneration

BMI: body mass index

CAS: carotid artery stenosis

CEA: carotid endarterectomy

CNS: central nervous system

CoW: Circle of Willis

CRT: central retinal thickness

CT: computed tomography

CTA: computed tomography angiography

DCP: deep capillary plexus

DSA: digital subtraction angiography

DUS: Doppler ultrasound

DVA: dynamic retinal vessel analysis

DVD: deep vessel density

EDI-OCT: enhanced depth imaging optical coherence tomography

eGFR: estimated glomerular filtration rate

ESVS: European Society for Vascular Surgery

FA: fluorescein angiography

FAZ: foveal avascular zone

fMRI: functional magnetic resonance imaging

fNIRS: functional near-infrared spectroscopy

GCC: ganglion cell complex

GEE: generalized estimating equations

HDL: high-density lipoprotein

ICA: internal carotid artery

LDL: low-density lipoprotein

MCA: middle cerebral artery

mfERG: multifocal electroretinography

MRI: magnetic resonance imaging

MRA: magnetic resonance angiography

NASCET: North American Symptomatic Carotid Endarterectomy Trial

NF: non-flow

NIRS: near-infrared spectroscopy

NO: nitric oxide

OCT: optical coherence tomography

OCTA: optical coherence tomography angiography

OD: optical density

PCoA: posterior communicating artery

RNFL: retinal nerve fiber layer

RPC: radial peripapillary capillary network

SCP: superficial capillary plexus

SD-OCT: spectral domain optical coherence tomography

SNR: signal-to-noise ratio

SQ: scan quality

SSADA: split-spectrum amplitude-decorrelation angiography

SSI: signal strength index

SVD: superficial vessel density

T: transmittance

TCD: transcranial Doppler

TIA: transient ischemic attack

VCI: vascular cognitive impairment

VD: vessel density

VEGF: vascular endothelial growth factor

λ: wavelength

1. Introduction

One of the major risk factors for cardiovascular and cerebrovascular diseases is aging, which is associated with increased prevalence and worsened prognosis of cardiovascular and cerebrovascular diseases. Carotid artery stenosis (CAS) is a potentially life-threatening consequence of systemic atherosclerosis in the aging population.

The disease affects a significant percentage of the aged population and is responsible for 10–20% of ischemic strokes, which are the second most common cause of death (1-3). Established risk factors that promote progressive atherosclerosis in the peripheral circulation may also exacerbate atherogenesis in the carotid arteries, leading to CAS. The most important risk factors for CAS are the following: age over 50 years, diabetes, hyperlipidemia, obesity, smoking, peripheral arterial disease, coronary disease, stroke or transient ischemic attack (TIA) in the medical history and occurrence of a cardiovascular event in a family member younger than 60 years (2).

Patients with CAS often present symptoms of cognitive impairment (2, 4-8). The pathogenesis of vascular cognitive impairment (VCI) related to CAS is complex. Severe CAS can reduce cerebral blood flow, leading to ischemic brain damage from hemodynamic insufficiency due to conditions like orthostasis, hypotension, or cardiac failure. Emboli from atherosclerotic lesions can also cause ischemic strokes in the supplied brain regions. Additionally, CAS is linked to microcirculatory dysfunction in the cerebral circulation, affecting smaller arterioles that regulate regional cerebral blood flow (9-12). Pathological changes in these vessels impact oxygen and nutrient supply to neuronal tissue, contributing to small vessel disease and promoting the formation of micro-infarcts (4, 13), white matter damage (14-17), and lacunar infarcts (18, 19), thereby exacerbating the pathogenesis of VCI. Furthermore, certain processes underlying the development of CAS also lead to pathological remodeling of the microcirculatory network (20-25) and microvascular rarefaction, impairing brain perfusion and contributing to VCI development (26). Endothelial cells also play a crucial role in regulating cerebral blood flow (26). The cerebromicrovascular endothelium modulates vascular tone and microcirculatory resistance by releasing vasoactive mediators like nitric oxide (NO) and prostaglandins (26, 27). Healthy endothelial function is essential for

adjusting regional blood flow to meet the energy demands of active neurons, a process called neurovascular coupling (26, 28-34). Impaired endothelium-mediated vasodilation in the cerebral microcirculation is directly linked to cognitive impairment (28, 29, 35). Pathological conditions associated with early CAS development (e.g., aging, hypercholesterolemia, hypertension, smoking, diabetes) cause significant endothelial dysfunction, leading to dysregulated cerebral blood flow (26).

A clear understanding of the microvascular manifestations of CAS is crucial for the prevention of cognitive decline and a reduction in cerebrovascular mortality among individuals at high risk for the disease. A variety of useful methods are available for studying the brain microcirculation and regulation of cerebral blood flow in humans. These include functional magnetic resonance imaging (fMRI)-based approaches and functional near-infrared spectroscopy (fNIRS). Given the limitations of many of these methods, including low resolution, high costs, long measurement times, time-consuming analyses, equipment availability, invasiveness, side effects of contrast agents, and so forth, there is an urgent need for sensitive, non-invasive methods that can be used in both large-scale cross-sectional studies and longitudinal studies to assess treatment efficiency.

The retina is anatomically an extension of the brain, having been formed as an outgrowth of the embryonic diencephalon during development. Consequently, the retina can be regarded as an extension of the central nervous system (36). The retinal and brain microcirculations share numerous anatomical and physiological characteristics, and the evidence strongly suggests that microcirculatory functional and structural alterations in the retina are closely correlated with those in the brain (37). Therefore, alterations of the retinal microcirculation are considered to represent changes in intracranial blood flow.

1.1. Carotid artery disease

1.1.1. Clinical characteristics

It is crucial to differentiate between asymptomatic and symptomatic CAS cases, as they are associated with disparate risk of stroke. The Asymptomatic Carotid Surgery Trial indicates that in asymptomatic cases with a degree of stenosis between 60–99%, the annual stroke risk is 0.7–1.1% per year (38). Cases are considered symptomatic when

beside a stenosis greater than 50% the patient has experienced symptoms indicative of stroke or TIA ipsilateral to the lesion within 6 months (39). Such symptoms include contralateral monoparesis or hemiparesis, paresthesia, dysarthria, dysphagia, aphasia, ipsilateral amaurosis fugax or blindness. The risk of a new stroke increases exponentially with the elapsed time since the presentation of the latest symptom. Within two days of a TIA, the probability of stroke increases to 6.7% (this level of risk is approximately equivalent to the 10-year accumulated risk for asymptomatic patients), and the stroke rate within two weeks is 10% (40). Consequently, secondary stroke prevention through carotid artery reconstruction exerts a more pronounced impact on reducing the risk of stroke when compared to asymptomatic patients. For this reason, clinical guidelines recommend carotid artery reconstruction within two weeks of a TIA or minor stroke, provided that there are no contraindications to surgery (41). The prevalence of stroke is significantly lower in patients who have undergone carotid endarterectomy (CEA) compared to those who have received pharmacological therapy (42, 43).

1.1.2. Role of the Circle of Willis (CoW) and Cerebral Collateral Blood Flow in Patients with Carotid Stenosis

The Circle of Willis (CoW) serves as the principal collateral pathway for maintaining perfusion in affected vascular territories. The anatomical features of the CoW significantly influence the clinical outcomes of carotid artery stenosis. Specifically, the anterior communicating artery (ACoA) and posterior communicating arteries (PCoA) are regarded as the primary collateral routes in patients with internal carotid artery (ICA) stenosis. Preferential flow patterns can develop, including collateral flow through the ACoA, the PCoA, or both. Previous studies examining computed tomography angiography (CTA) scans of patients who underwent carotid artery reconstruction found a significantly higher prevalence of CoW variants in patients with substantial carotid artery stenosis compared to a healthy control group. Additionally, absent or hypoplastic segments were more frequently observed among patients with stroke. Other collateral vessels, such as leptomeningeal collaterals and extracranial-to-intracranial collaterals (e.g., retrograde flow in the ophthalmic artery), are recognized as secondary cerebral collateral blood flow pathways. Additionally, cortical anastomoses extend between the terminal branches of the cerebral arteries at the cortical surface and into the

leptomeningeal space, just before the pial arteries penetrate the gray matter. A collateral supply system also exists between the external carotid artery and the ICA.

1.1.3. Current protocols of carotid artery stenosis management

1.1.3.1. Diagnosis

In the current clinical practice, duplex ultrasound is the most commonly employed method for diagnosing and evaluating the severity of carotid artery stenosis. This rapid, cost-effective, and highly precise method provides not only morphological data but also enables the evaluation of the extent of the stenosis by measuring the different flow velocities. Although Doppler ultrasound (DUS) can be a reliable examination method when performed by an experienced examiner, previous studies have demonstrated that several human factors can increase error and variability (44, 45). Computed tomography- and magnetic resonance angiography (MRA) are more objective than DUS. The latter imaging methods are primarily used in reconstruction planning due to their capacity to provide suitable images of the blood vessels from the aortic arch to the intracranial vessels and the ischemic lesions of the skull (Figure 1). The degree of stenosis in CTA and MRA is calculated according to the criteria developed by the North American Symptomatic Carotid Endarterectomy Trial (NASCET) (43), which compares the residual lumen at the most stenotic portion of the proximal ICA to the normal diameter of the distal post-stenotic ICA.

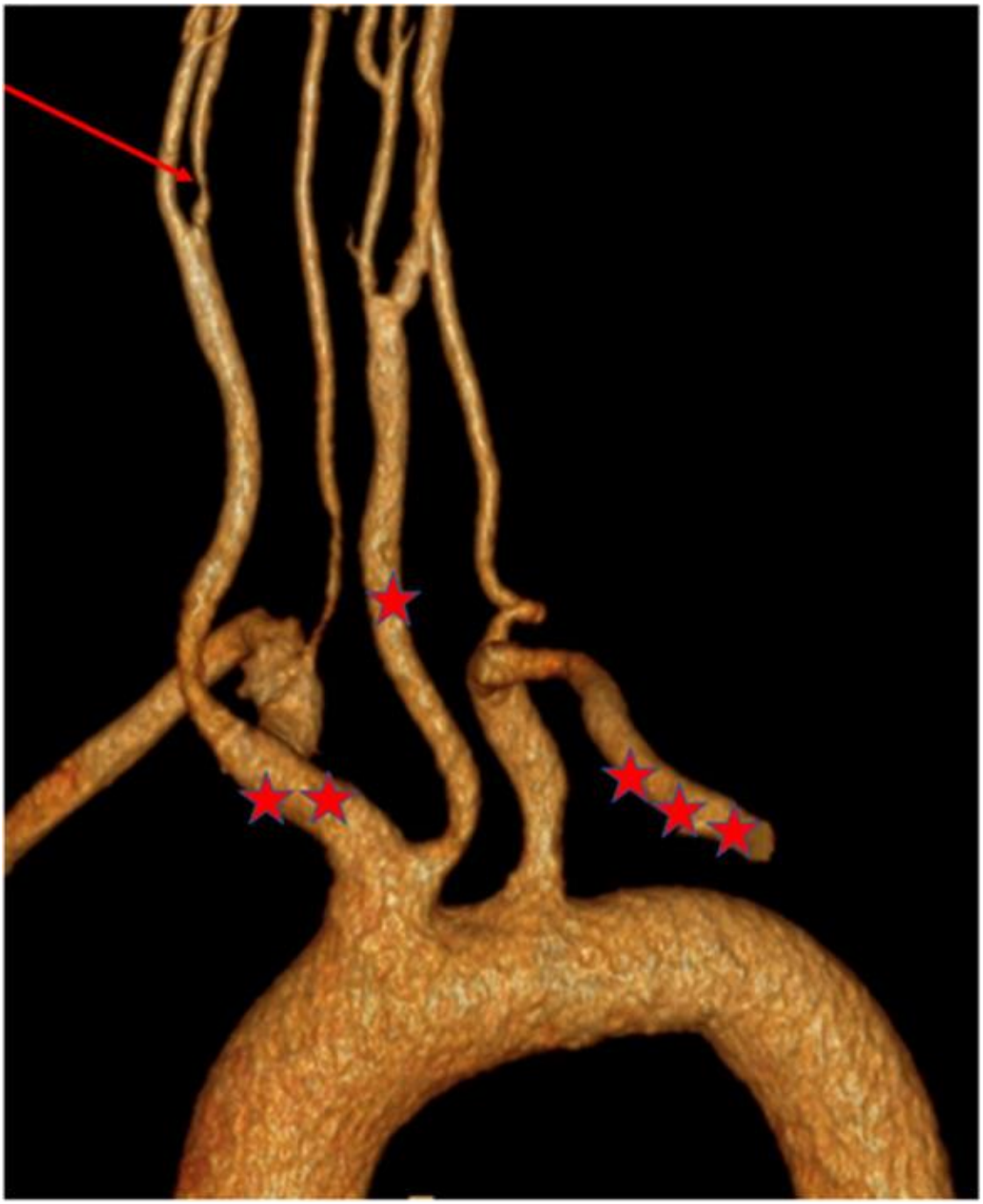

Figure 1. The 3D reconstruction of CT angiography illustrates the supra-aortic branches of the aorta. One red asterisk marks the brachiocephalic trunk, which divides into the right common carotid and subclavian arteries. The red arrow indicates significant stenosis in the right internal carotid artery distal to the carotid bifurcation. Two red asterisks denote the left common carotid artery, while three red asterisks highlight the second part of the left subclavian artery, distal to the origin of the left vertebral artery. Image of our working group, published in (46).

Conventional Digital Subtraction Angiography (DSA) is not considered first-line for assessing carotid stenosis. Unless there are significant discrepancies with noninvasive imaging (e.g., DUS, CTA, or MRA), it should not be performed in patients who are candidates for revascularization.

If carotid endarterectomy is being considered, it is recommended that the DUS stenosis estimate be confirmed by CTA or MRA, according to the European Society for Vascular Surgery (ESVS) guideline (41). If CAS is being considered, CTA or MRA to provide additional information on the aortic arch and the extra- and intracranial circulation is also recommended to follow any DUS study.

Although these imaging modalities are effective in clinical practice and allow evaluation of the degree of stenosis, the effect on downstream CNS microcirculation cannot be assessed.

1.1.3.2. Treatment

In asymptomatic cases, when the degree of stenosis is less than 70%, pharmacological treatment is recommended, as well as the reduction of modifiable risk factors (41). A case is considered to be asymptomatic if there has been no stroke, TIA or other neurological symptom related to the stenosis within six months. Medical therapy is based on antiplatelet agents, lipid lowering therapy and the treatment of comorbidities such as diabetes and hypertension (47). For patients with asymptomatic carotid stenosis exceeding 50%, a lower dose of aspirin (75-325 mg daily) should be considered, primarily for the prevention of late-onset myocardial infarction and other cardiovascular events. Lipid lowering therapy with statins, either alone or in combination with ezetimibe, is recommended for the long-term reduction of the risk of stroke, myocardial infarction, and other cardiovascular complications. Hypertension is a known risk factor for the development of asymptomatic carotid stenosis, and effective treatment of this condition in adults has been demonstrated to slow the progression of stenosis. Patients with diabetes are at an increased risk of developing stroke, with 20% of this population dying as a result. Diabetes is associated with a higher prevalence of asymptomatic carotid stenosis, hypertension, and an abnormal lipid profile. Therefore, treatment of the condition is essential. Pharmacologic treatment is also the preferred alternative when the risk of

intervention is considered too high compared to its potential preventive value. Concerning surgical treatment options, the first line of treatment is endarterectomy, as this procedure has the lowest perioperative stroke rate (48, 49). The procedure consists of removing the calcified endothelium and the median layer of the vessel, which can be performed under general or locoregional anesthesia. The two ways of performing the procedure are conventional endarterectomy, which involves closing the wound with a patch angioplasty, and eversion endarterectomy, which involves everting the intima and media layers. The advantage of the latter approach is that it is free of non-autologous material. This means less infection and patch degeneration, as well as lower postoperative embolization and restenosis rates. In cases where the perioperative risk is considered too high, where the patient has a history of previous cervical surgery or radiation, and in cases of restenosis and contralateral recurrent nerve palsy, carotid angioplasty and stent implantation followed by lifelong medical therapy is the preferred treatment. Lifelong use of statins and thrombocyte aggregation inhibitors after surgery is essential, as are regular ultrasound examinations (41).

1.2. Ocular manifestations of carotid artery disease

As the eye receives its blood supply from the ophthalmic artery derived from the ipsilateral internal carotid artery, CAS can result in severe ophthalmic complications. In the presence of ocular abnormalities, carotid stenosis is considered symptomatic. Temporary reductions in blood flow can cause a painless unilateral transient vision loss, which is termed amaurosis fugax. It is a type of TIA caused by an embolus derived from the ipsilateral atherosclerotic carotid artery, which transiently occludes the retinal arteries, causing retinal hypoxia (50). In cases of severe CAS, amaurosis fugax can also result from retinal hypoperfusion when the retina is exposed to intense light, and its metabolic needs exceed what can be met through functional hyperemia (51). The duration of vision impairment may vary considerably, from seconds to minutes. In rare cases, it can last for hours and resolve spontaneously. Embolization of the retinal arteries can also lead to a sudden, painless, and permanent loss of vision caused by a retinal stroke. Depending on the size of the emboli and the location of the stenosis, this can manifest as visual field defects or total vision loss in one eye if the central retinal artery is affected. The consequences of retinal infarction can be observed in the posterior segment of the eye.

During the acute phase, there is a whitening of the affected areas of the retina, which is a consequence of intracellular edema. A cherry red spot can be seen in the fovea due to the visibility of the underlying normal choroidal circulation. This change is the most notable and later resolves. In approximately half of the cases, retinal emboli may be identified on funduscopic examination (Figure 2) (52). Retinal artery occlusion is considered an acute medical emergency that requires immediate referral to the nearest stroke center to minimize the chance of associated cerebral circulatory disturbance or myocardial infarction. A blockage that persists for a period longer than four hours results in irreversible vision loss (53). The objective of treatment within this window of time is to preserve optimal vision. In the absence of systemic contraindications, the initial treatment of choice is systemic tissue plasminogen activator. Studies suggest that this treatment enhances long-term visual outcomes (54). In case this is contraindicated, conservative therapy, such as ocular massage, anterior chamber paracentesis, and topical intraocular pressure reduction, is considered an alternative. Systemic conservative treatment with beta-blocking agents, sublingual isosorbide, or inhalation of high concentrations of oxygen is a further possible option. These treatments are aimed at inducing vasodilation, which results in the migration of the embolus toward the periphery (55). Retinal embolization is associated with an increased risk of stroke (56-58), thereby confirming the shared etiologies of vascular pathologies affecting the brain and the retina.

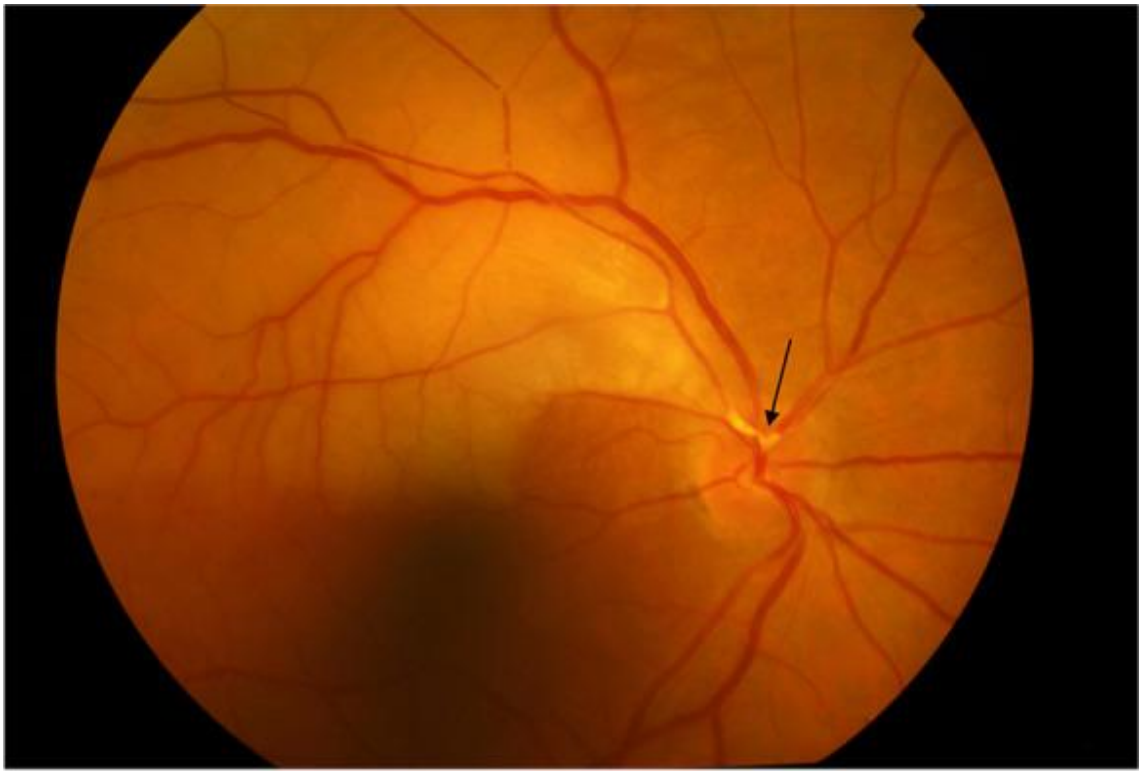

Figure 2. Branch retinal artery occlusion exhibiting retinal whitening in the affected area, caused by a calcified embolus on the color fundus photograph (arrow). Own image, published in (46).

If the stenosis is not treated, ocular ischemic syndrome can develop. In these cases, vision loss develops gradually and is accompanied by severe pain. Ocular findings include changes in the anterior segment, such as neovascularization in the iris and the iridocorneal angle, opalescence of the aqueous humor, as well as in the posterior segment, where narrowed retinal arteries and dilated retinal veins, retinal hemorrhages, microaneurysms, or a cherry-red spot in the macula can appear (Figure 3). The management of ocular ischemic syndrome is always a multidisciplinary task; in addition to ophthalmologic care, systemic treatment is also required. From an ophthalmic point of view, the most important task is to control complications (59). Retinal ischemia leads to the production of vascular endothelial growth factor, which subsequently causes the neovascularization. The growth of blood vessels in the anterior segment leads to neovascular glaucoma, which is often resistant to treatment. The likelihood of this can be reduced by panretinal photocoagulation. If the posterior segment is not visible, transconjunctival cryotherapy or trans-scleral diode laser retinopexy may be considered. For existing neovascular

glaucoma, medical therapy (beta-blocker or alpha-2 agonist eye drops and topical or per os carbonic anhydrase inhibitors) or, if this is ineffective, surgical treatment (trabeculectomy or shunt implantation) is considered. If these treatments are not sufficient, the possibility of enucleation should also be considered in the case of persistent and severe pain.

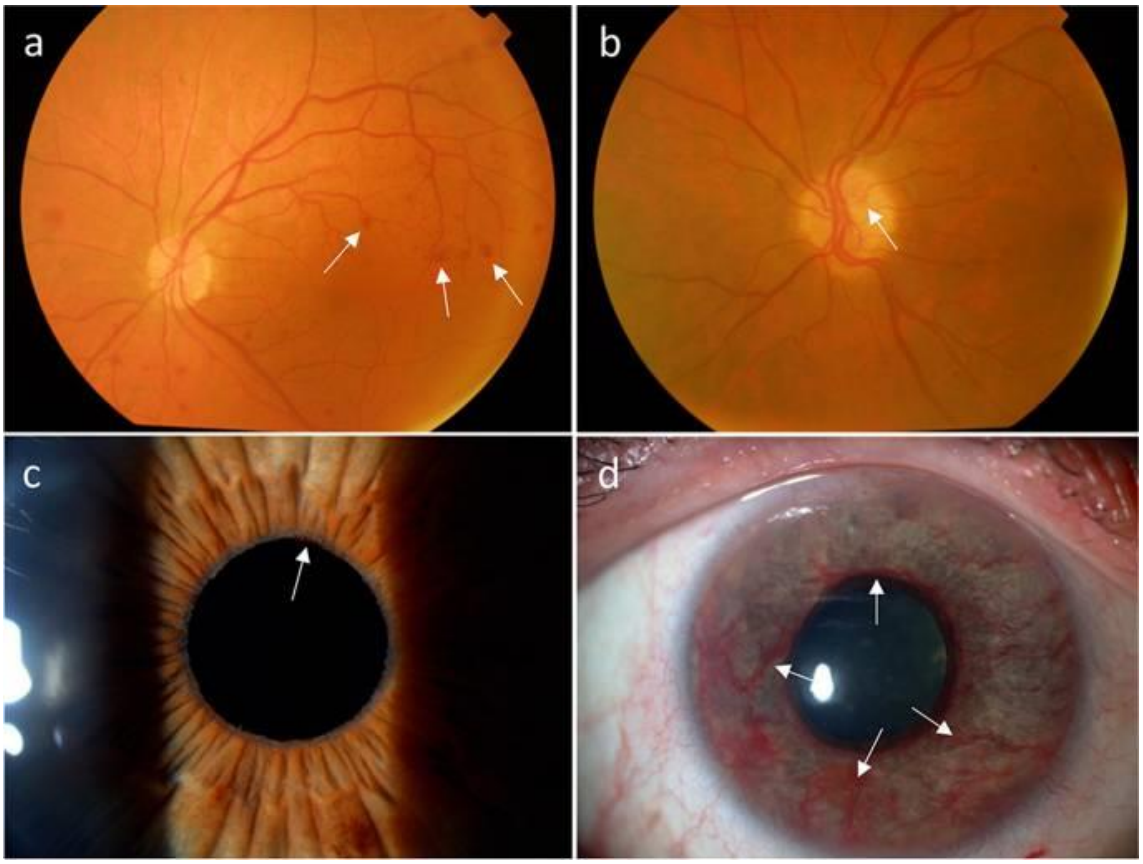

Figure 3. Pathological changes in the retina (a, b) and anterior segment of the eye (c, d) resulting from ocular ischemic syndrome. Retinal dot hemorrhages (a, arrows), and neovascularization of the optic nerve head (b, arrow) signify severe retinal ischemia. Chronic ocular ischemia progresses to anterior segment neovascularization, initially at the pupillary margin (c, arrows), and subsequently on the surface of the iris (d, arrows). Own image, published in (46).

CAS is also associated with the occurrence of retinal vein occlusion (60). As a result of atherosclerosis, a stiff-walled artery can block the underlying vein, leading to a branch retinal vein occlusion. Symptoms depend largely on the location of the blockage and the size of the affected area. Most commonly, the main complaint is a sudden, painless loss

of vision or visual field loss. On the fundus, abnormalities are typically seen in a wedge-shaped arrangement corresponding to the supply area of the occluded vein; the most common abnormalities are flame-shaped hemorrhages, dot and blot hemorrhages, cotton wool spots, and dilated, tortuous veins. Prolonged persistence without treatment leads to neovascularization in both the posterior and anterior segments, which may result in hemorrhage or secondary glaucoma. The mainstay of ophthalmologic treatment is sectoral laser treatment of the ischemic area and intravitreal anti-vascular endothelial growth factor (anti-VEGF) injections to prevent neovascularization and intravitreal steroid treatment for macular edema (61).

1.3. Imaging retinal structures and the retinal microvasculature in CAS patients

1.3.1. Understanding microvascular pathologies associated with CAS by examining the retinal microvasculature

The retinal microvasculature offers a distinctive opportunity to investigate the pathogenesis of cerebral small vessel disease, given its similarities in anatomy, physiology, and embryology to the cerebral circulation. Direct visualization of retinal vessels using the methodologies outlined below offers a possibility for studying retinal microvascular health, which may be considered a proxy for cerebral microvascular health in patients diagnosed with CAS.

The retinal and choroidal vasculature provide blood supply to the retina. Both originate from the ophthalmic artery, the initial branch of the internal carotid artery. Consequently, alterations in blood flow within the internal carotid artery may result in ophthalmic complications. Additionally, pathophysiological changes affecting both the CNS and cerebral microcirculation impact the retina and retinal microcirculation through common cellular, molecular, thromboembolic, and hemodynamic mechanisms. Moreover, the retina may serve as an area of the CNS where pathological alterations in tissue structure can be directly visualized for diagnostic purposes. The metabolic activity of the retina is high, and it has one of the highest oxygen demand among the organs. Furthermore, retinal and cerebral microcirculation have several common features, including end arteries without anastomoses, a barrier, and autoregulatory role, and the characteristics of low-flow/high-oxygen-extraction systems (62). Similarly to the brain, the retina has minimal

local oxygen and energy reserve capacity, necessitating functional hyperemia to fulfill the demands of activated neurons. Dynamic regulation of regional blood flow in areas of neuronal activation occurs via neurovascular coupling, with the retina being the only CNS region where this phenomenon can be directly assessed (63).

Several methods exist for imaging the ocular circulation, including funduscopy and fluorescein angiography (FA). FA is an invasive diagnostic procedure used to assess retinal circulation. It assists in diagnosing various ocular pathologies and helps in planning the management of ocular diseases. However, these methods do not provide the quantitative measurement of the blood supply. Doppler ultrasound imaging of ocular arteries provides greater insight into the retinal microcirculation than traditional angiography. Nevertheless, it is limited to the larger ocular arteries and thus less informative for the detailed study of the retinal microcirculation. Some more recent techniques can provide more accurate functional measurements. Optical coherence tomography (OCT) offers high-resolution, cross-sectional morphological imaging of the retina and the choroid, while optical coherence tomography angiography (OCTA) is capable of imaging the retinal vasculature by detecting the movement of red blood cells in consecutive scans. Furthermore, a novel method, dynamic retinal vessel analysis (DVA), permits the investigation of the dynamic regulation of the retina's blood supply in response to neuronal activation induced by flickering light (64, 65). However, this examination method is not yet widely used in clinical practice and is mainly used in trials.

1.3.2. Fluorescein angiography

For several decades, FA has been the gold standard for visualizing retinal circulation. This dye-based imaging technique involves the injection of fluorescein dye into a peripheral vein in the arm or hand, followed by the illumination of the retina with blue light. The emitted fluorescent green light is recorded to create an image of the retinal vasculature. FA enables the dynamic evaluation of contrast movement in real-time. Although it is generally a safe procedure, it is associated with potentially life-threatening adverse effects. It provides information regarding not only retinal vascular perfusion but also the integrity of the inner blood-retinal barrier. It is possible to obtain images of the peripheral retina as well as the posterior pole of the eye. One disadvantage of FA is that it is unable

to provide quantitative data about the retinal blood supply. In addition, it does not allow for depth perception, but only gives a two-dimensional picture.

1.3.3. Doppler ultrasonography of the ophthalmic artery

Doppler imaging has been utilized for a long time for imaging of orbital structures. Color Doppler imaging provides a real-time representation of blood flow in a color-coded format. This method is suitable for examining the ophthalmic artery, the posterior ciliary artery, and the central retinal artery (66). However, it cannot provide functional information regarding retinal microcirculation, which limits its utility for assessing microcirculatory complications of the disease.

1.3.4. Optical coherence tomography

OCT is a rapid, non-invasive, and non-contact imaging technique that allows in vivo visualization of retinal structures, the optic nerve head, and the retinal nerve fiber layer (RNFL) through low coherence interferometry (67). Since its introduction in 1991, OCT has become a widely utilized diagnostic and longitudinal follow-up tool for retinal diseases such as age-related macular degeneration (AMD), diabetic retinopathy, and glaucoma (68, 69). OCT enables the acquisition of high-resolution cross-sectional images, which provide clear visualization and measurement of the thickness of retinal layers. Unfortunately, the contrast between retinal vessels and the surrounding tissue is not sufficient for discerning vascular structure. As a result, retinal OCT is unsuitable for directly monitoring retinal blood flow changes. Still, it can effectively detect the consequences of impaired retinal blood flow, such as edema in acute cases and retinal atrophy in the long term.

1.3.5. OCT angiography

OCTA represents a novel method for visualizing and analyzing the retinal and choroidal vasculature, as it is able to do so without the use of an intravenously administered dye. The imaging technique is based on the temporal changes of OCT signals with motion contrast technology, enabling the detection of the movement of red blood cells within the vessels. This technology allows for the precise visualization of the microvasculature of the macular area and around the optic disc, as well as the provision of quantitative data,

including vessel density (VD) and the size of the foveal avascular zone (FAZ). VD is calculated as the ratio of the detected vessels to the whole image. The detection of the different capillary layers is based on automatic segmentation, which can be manually adjusted in case of inaccuracy. Projection artifacts in OCTA occur when superficial retinal flow signals are reflected by deeper layers, leading to false detection of blood flow in deeper structures; although built-in software can mask these artifacts, it has limitations, especially in hyperreflective pathological areas. Examination of the cross-sectional OCTA scan is recommended to distinguish true flow from artifacts (70). To calculate the FAZ, the instrument automatically displays the boundaries of the capillary free zone in the central part of the macula and then quantifies the size of the selected area in mm^2. If the selection is incorrect, manual correction is possible. The examination is rapid and easily repeatable, with the additional benefit of providing simultaneous structural and functional blood flow information. It should be noted that the method has certain limitations. For instance, the smallest capillaries, where the velocity of blood cells is below the detectable threshold, cannot be visualized. Similarly, bleeding and leakage cannot be seen either. The current OCT devices and software are only capable of measuring the central parts of the retina, specifically a 3–8 mm square of the macular area or a 4.5–6 mm square of the peripapillary area. The most significant constraints on OCTA are those that affect image quality, including media opacities and various artifacts resulting from blinking or saccadic eye movements. Previous studies have demonstrated the significance of image quality in influencing measurement error, with scans exhibiting lower quality scores exhibiting a markedly higher degree of error (71-75). The image quality of OCT scans is evaluated through various indicators derived directly from the raw optical signal (interferogram) captured by the device. Different commercially available OCT devices have specific acceptance ranges and thresholds recommended by manufacturers (76). SSI and Scan Quality (SQ) index are automated quality indices generated by the RTVue-XR AngioVue software versions 6.5 and 7.0, respectively. In this study, the AngioVue software (version 2017.1, phase 7 update) provided with the RTVue-XR Avanti System utilizes the SQ index as a measure of image quality. Although the exact formulation of SQ is undisclosed, this unitless parameter offers an objective scalar value ranging from 0 to 10 (where higher values indicate better quality), considering errors arising from eye motion, defocus, and signal-to-noise ratio. The intensity of reflected light

influences the latter during scanning and various optical/electronic noise factors. The recommended threshold for acceptable image quality with the AngioVue system is an SQ score of 6 or higher. Nevertheless, the non-invasive nature of OCTA is a significant advantage, and its use is rapidly expanding in clinical practice. For instance, OCTA is employed for the early detection of microvascular alterations in diabetic retinopathy, the visualization of the boundaries of nonperfusion in vascular occlusion, and the monitoring of patients with AMD. Furthermore, OCTA is a promising tool for diagnosing and monitoring glaucoma.

2. Objectives

Our research aimed to confirm the effect of image quality on vascular network density measurements and, using this result, investigate the OCT angiography parameters in patients with carotid stenosis, with a particular focus on the effect of endarterectomy on vascular network density. We also investigated the association between the OCT angiographic parameters and the morphology of the Circle of Willis.

2.1. Assessing how signal quality affects OCTA measurements

In this study, we examined the impact of deterministic signal loss on OCTA image quality and measurements using the RTVue-XR Avanti System. Our ultimate objective was to establish the relationship between the SQ index and the measured angiographic parameters and to develop a correction factor to account for variations in the SQ value during patient follow-up.

2.2. Evaluation of the influence of systemic factors on OCTA measurements in patients with carotid artery stenosis

To examine the impact of systemic risk factors as well as carotid endarterectomy on retinal blood flow parameters in the eyes of patients with significant carotid artery stenosis, utilizing OCT angiography before and after carotid endarterectomy. Additionally, the correlation between CoW morphology and OCTA characteristics was investigated.

3. Methods

3.1. Studying the effect of signal loss on OCTA parameters

3.1.1. Study design and subjects

In this prospective, observational, cross-sectional study, a total of 30 eyes from 15 healthy subjects (6 male and 9 female, mean age: 34.33 ± 13.22 years) from the outpatient clinic of the Department of Ophthalmology at Semmelweis University were included. The study was conducted in accordance with the Declaration of Helsinki and relevant national and local requirements and was approved by the National Drug Agency's Ethical Review Board for Human Research (OGYÉI/20606/2017). All subjects provided written informed consent. Each subject underwent a comprehensive ocular examination to ascertain their ocular health. Subjects with a greater refractive error than 6 diopters were excluded.

3.1.2. Ophthalmological examinations

Optical coherence tomographic angiography imaging was conducted using the AngioVue OCTA system with a split-spectrum amplitude-decorrelation angiography (SSADA) software algorithm (RTVue XR Avanti with AngioVue, Optovue Inc, Fremont, California, USA). The AngioAnalytics software of the AngioVue system, which employs an automated segmentation algorithm, was utilized to assess superficial vessel density (SVD) and deep vessel density (DVD) in the central 3 × 3 mm macular region and the 4.5 × 4.5 mm peripapillary area. Furthermore, the software evaluated the size of the FAZ and non-flow (NF) area at the level of the superficial capillary plexus, in addition to measuring the central retinal thickness (CRT) and peripapillary RNFL thickness. Segmentation errors were meticulously checked on each B-scan during the image selection process. Consequently, only those OCTAs with an accurate segmentation at the superficial and deep vascular plexus level were selected for further analysis. Scans with autosegmentation alignment errors at the level of the retinal plexuses, images with double vessel patterns, significant dark areas from blinks, white line artifacts, and vessel discontinuities induced by microsaccades, as well as shadowing and projection artifacts were excluded.

Light filters with different characteristics were used during the tests in order to simulate the image degradation observed in a clinical setting. The attenuation of light by an optical filter can be quantified by its optical density (OD), which depends on the wavelength (λ). The fraction of light power that passes through the filter is the transmittance (T). and OD is defined as OD = −log (T). As the central wavelength of the OCT light source is λ = 840 nm, and the typical spectral width of such a superluminescent diode is approximately 40 nm, the filters utilized in this study (an uncoated absorptive neutral density filter, Edmund Optics Ltd., Barrington, NJ, USA) were measured in the 820 to 860 nm wavelength range by a Perkin-Elmer Lambda 35 spectrophotometer. The obtained average T and OD values are listed in Table 1. OCTA scans were acquired under standardized dim light conditions, thus excluding the influence of pupil size on image quality. All subjects underwent two image acquisitions (one macular and one optic disc scan), both performed without the absorptive filter and with two randomly selected absorptive filters in random order. When utilizing the filters, an approximately 10-degree tilted position was employed to prevent the reflection of light from the filters back into the instrument. Absorptive filters, in the form of glass plates with thicknesses ranging from 0.76 to 2.90 mm, can alter the optical path length, similar to measuring a strongly myopic eye, impacting OCT scan quality. To exclude the influence of elevated optical path length on the deterioration of the image, scans were conducted with the insertion of a clear glass plate (Schott B270 glass) of 2 mm thickness – which is close to that of the absorptive filters – between the equipment and the eye. The SQ values from these scans were then compared to those obtained without the glass plate. All measurements were conducted by the same experienced examiner. The SQ value of each scan, as provided by the AngioVue software, was collected in order to quantify the OCTA image quality. For statistical analysis, only those images with an SQ score of at least 5 were included.

3.1.3. Statistical analysis

A priori sample size calculation for one-sample t-test (power = 0.90; P = 0.05; clinically important difference in SQ = 1) indicated that a minimum of 20 eyes of 10 subjects were needed to provide reliable statistical results. Therefore, the final sample size of 30 eye samples from 15 subjects was selected to ensure reliable statistical results. A multivariable regression on repeated measures via generalized estimating equations

(GEE) model was employed to assess the correlation between SQ values and OD of filters, in addition to the effect of attenuated image quality on OCTA parameters. In this model, measurement data acquired with and without absorptive filters from the two eyes of one subject were statistically analyzed as repeated measures. Consequently, this analysis takes into account the correlated nature of data obtained from two eyes of the same patient, thus providing valid *p*-values for mean changes in OCTA parameters from repeated measurements. For all analyses, a *p*-value of less than 0.05 was deemed to be statistically significant.

3.2. Assessment of the impact of systemic factors on OCTA measurements in patients with carotid stenosis

3.2.1. Study design and subjects

A total of 56 patients with significant carotid artery stenosis were enrolled in this prospective clinical study, all of whom were being prepared for carotid endarterectomy at the Department of Vascular and Endovascular Surgery of Semmelweis University. The study followed the tenets of the Declaration of Helsinki, applicable national and local regulations, and was prospectively approved by the Ethical Review Board for Human Research of the National Drug Agency (OGYÉI/20606/2017). Written informed consent was signed by all participants.

Inclusion criteria were significant carotid artery stenosis (≥70%) and planned endarterectomy. None of the patients had CAS-related ocular symptoms or findings. Exclusion criteria were associated ocular diseases (such as age-related macular degeneration, glaucoma, and vitreomacular disease), previous intravitreal anti-VEGF injections, and the presence of clinically significant media opacities.

The severity of carotid artery stenosis was assessed by computed tomography angiography as part of the clinical routine. All patients with carotid artery disease underwent preoperative unenhanced cranial 256-slice CT. CTA of the carotid arteries was performed from the level of the aortic arch to the vertex with bolus tracking (Brilliance iCT 256, Philips Healthcare, Best, The Netherlands). For data acquisition, the following imaging parameters were used: 120 kV, 50–160 mAs/slice, slice thickness 0.67 mm,

Philips® IMR reconstruction, intravenous contrast (Iomeron400), 50 ml at a flow rate of 5 ml/sec.

3.2.2. Surgical procedure

Surgical treatment was carried out at the Department of Vascular and Endovascular Surgery, Semmelweis University. Carotid artery reconstruction was performed under general anesthesia in all patients. During surgery, a longitudinal incision is made parallel to the medial border of the sternocleidomastoid muscle. The carotid sheath is entered, and the medial border of the jugular vein is dissected. All patients underwent eversion endarterectomy, which is performed with complete transection of the bifurcation, followed by eversion of the adventitia and mobilization upward while applying gentle caudad traction to the plaque. The divided bifurcation is reunited with a simple end-to-end anastomosis after endarterectomy. Near-infrared spectroscopy (NIRS) was used for cerebral monitoring.

3.2.3. Ophthalmological examinations

Each subject underwent three imaging sessions, during which three consecutive OCTA images of the macular area and the optic disc were obtained. The first session was performed during the perioperative period, and the other two were performed during the first postoperative week and one month after surgery. The ophthalmic visits consisted of visual acuity testing, slit-lamp biomicroscopy including fundus examination, followed by optical coherence tomography angiography. OCTA imaging was performed under the same conditions by a trained examiner. The AngioVue device with an SSADA software algorithm (RTVue XR Avanti with AngioVue, Optovue Inc, Fremont, California, USA) was used. The device acquires 70.000 A-scans per second in approximately 3.0 seconds. Macular imaging required a 3 × 3 mm scan because the current version of the AngioAnalytics software obtains the highest resolution scans in the central 3 mm diameter. Images with motion artifacts (such as vessel doubling, white line artifacts, vessel discontinuities, or noise), projection artifacts, and segmentation errors were excluded. Scan quality was required to be greater than SQ 5, and images with an SQ of 5 or less were also excluded.

3.2.4. Brain CT and CTA examinations and evaluation

All CT imaging scans were conducted with a 256-slice scanner (Brilliance iCT 256, Philips Healthcare, Best, The Netherlands). A brain CT scan was performed in accordance with the institutional protocol, utilizing the following parameters: field of view 200–250 mm, collimation 64 × 0.625, pitch 0.39, gantry rotation time 400 ms, tube voltage 120 kVp, tube current 120–204 mAs, slice thickness 2 mm, dose-length product 312–626 mGycm. A contiguous reconstruction was performed with a slice thickness of 0.67 mm and a 512 × 512 matrix, utilizing iterative model reconstruction (IMR, Philips Healthcare, Cleveland, OH, USA). Thin-section images were subsequently analyzed on an IntelliSpace Portal workstation (Philips Healthcare, Best, The Netherlands), which included maximum intensity projection slabs with a thickness of 3 mm, oriented both parallel and perpendicular to the anterior skull base. This methodology was utilized to achieve a comprehensive overview of the Circle of Willis. The CoW was assessed according to a previously established evaluation protocol (77). Each segment was classified as normal (diameter ≥0.8 mm), hypoplastic (< 0.8 mm), or non-visualized.

3.2.5. Statistical analysis

For statistical analysis, SPSS software (version 23.0, IBM, Armonk, NY, USA) was used. The effect of systemic parameters and image quality on OCTA parameters was assessed with multivariable regression analysis using the GEE model. In addition to handling repeated measures (within-session and between-visit), this test allows adjustment for within-subject correlation of parameters (right vs. left eye) by taking into account between-eye correlations. In addition, their effect on the dependent variables can be controlled by including scan quality and risk factors as covariates in the GEE model. Age, degree of stenosis in %, aspirin use, clopidogrel use, body mass index (BMI), eGFR, serum cholesterol, low-density lipoprotein (LDL), high-density lipoprotein (HDL), and triglyceride levels, in addition to the presence of hypertension and diabetes, were evaluated as potential confounders. The effect of systemic predictors on OCTA parameters was analyzed in bivariable models (adjusting for scan quality for each predictor), and statistically significant predictors were entered into multivariable models.

4. Results

4.1. Effect of deterministic signal loss on OCTA measurements

Without the absorptive filter, SQ values ranged from 5 to 9, with an overall mean of 8.25 ± 0.95. Figures 4 and 5 illustrate the notable effect of light attenuation on macular and peripapillary VD measurements.

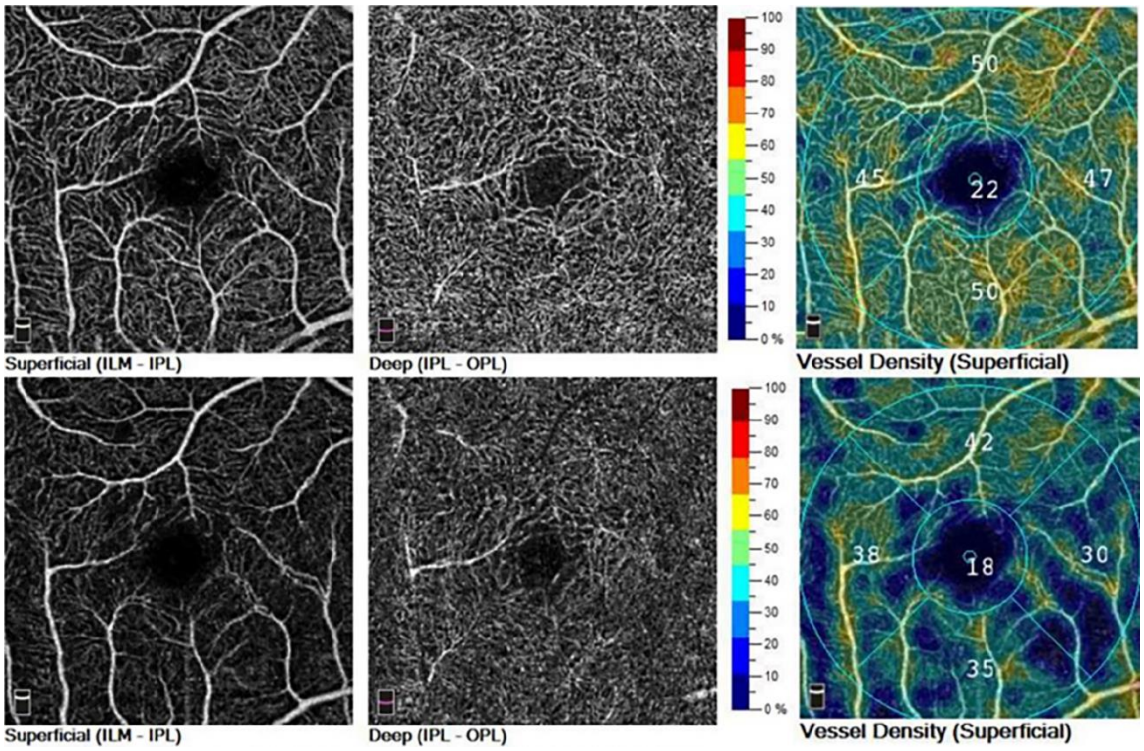

Figure 4. En face OCTA imaging of the superficial (SCP) and deep retinal capillary plexus (DCP), along with SCP vessel density (VD) (SQ = 9, top row) and by decreasing light transmittance through the use of an absorptive optical filter OD 0.25 (SQ = 6, bottom row) in the same healthy subject. In scans with lower image quality, the retinal microvasculature appears less visible in general, and focal areas of vascular attenuation and a significant reduction in SCP VD are also evident. Own image, published in (78).

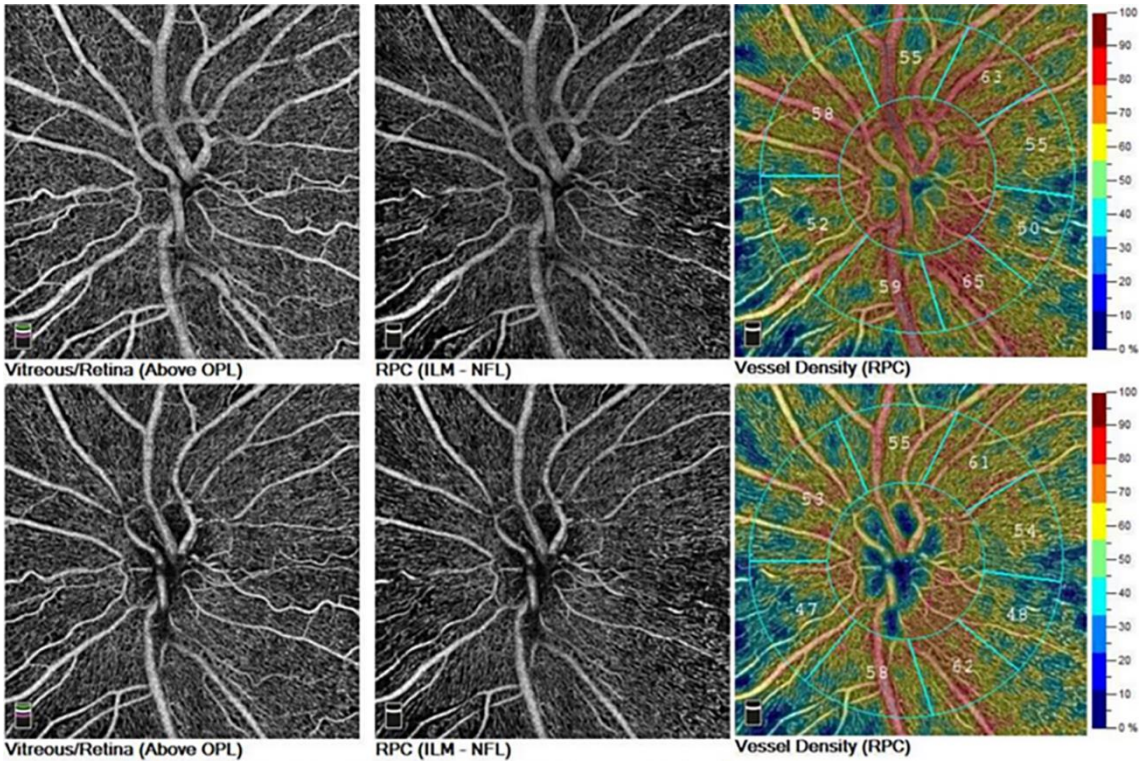

Figure 5. En face OCTA imaging of the optic nerve head, along with radial peripapillary capillary VD, was conducted with an SQ of 8 (top row) and after reducing light transmittance using an absorptive optical filter OD 0.13, resulting in an SQ of 7 (bottom row) in the same healthy subject. The scans with lower image quality not only showed a general reduction in the visibility of the optic disc and peripapillary microvasculature but also exhibited a significant reduction in RPC VD. Own image, published in (78).

Introducing a 2.0-mm-thick glass plate between the OCT device and the eye did not result in a significant change in SQ values, supporting the hypothesis that an increased optical path does not affect image quality (Table 1). However, comparing SQ values from the reference measurement without attenuated image quality indicated a significant negative effect of absorptive filters with decreasing light transmittance on the corresponding SQ values (Table 1).

Table 1. Average change in OCTA scan quality resulting from signal loss when absorptive filters with decreasing optical transmittance are placed in front of the eye during measurement

	Optical quality			Change in scan quality (SQ)			
	Optical density	**Light transmittance**	**Filter thickness**	**Mean**	**SE**	**95% CI**	***p***
No filter	**0** (n = 60)	100%	-	-	-	-	-
Glass plate	**0.04** (n = 30)	91.7%	2.0 mm	-0.10	0.07	-0.28 – 0.08	0.17
Absorptive filter*	**0.09** (n = 30)	81.9%	0.76 mm	-0.57	0.15	-0.18 – -0.96	<0.001
	0.13 (n = 30)	74.9%	1.20 mm	-1.00	0.20	-0.49 – -1.55	<0.001
	0.25 (n = 30)	56.6%	2.90 mm	-1.33	0.12	-1.02 – -1.64	<0.001
	0.36 (n = 30)	43.8%	2.50 mm	-1.71	0.14	-1.35 – -2.07	<0.001

Subsequently, a regression analysis was conducted between the light transmittance of different filters and the corresponding SQ values of the scans, revealing a strong correlation ($r = 0.53$; $p < 0.001$; Figure 6). Lower scan quality in OCTA images was associated with decreased retinal VD (Figure 7).

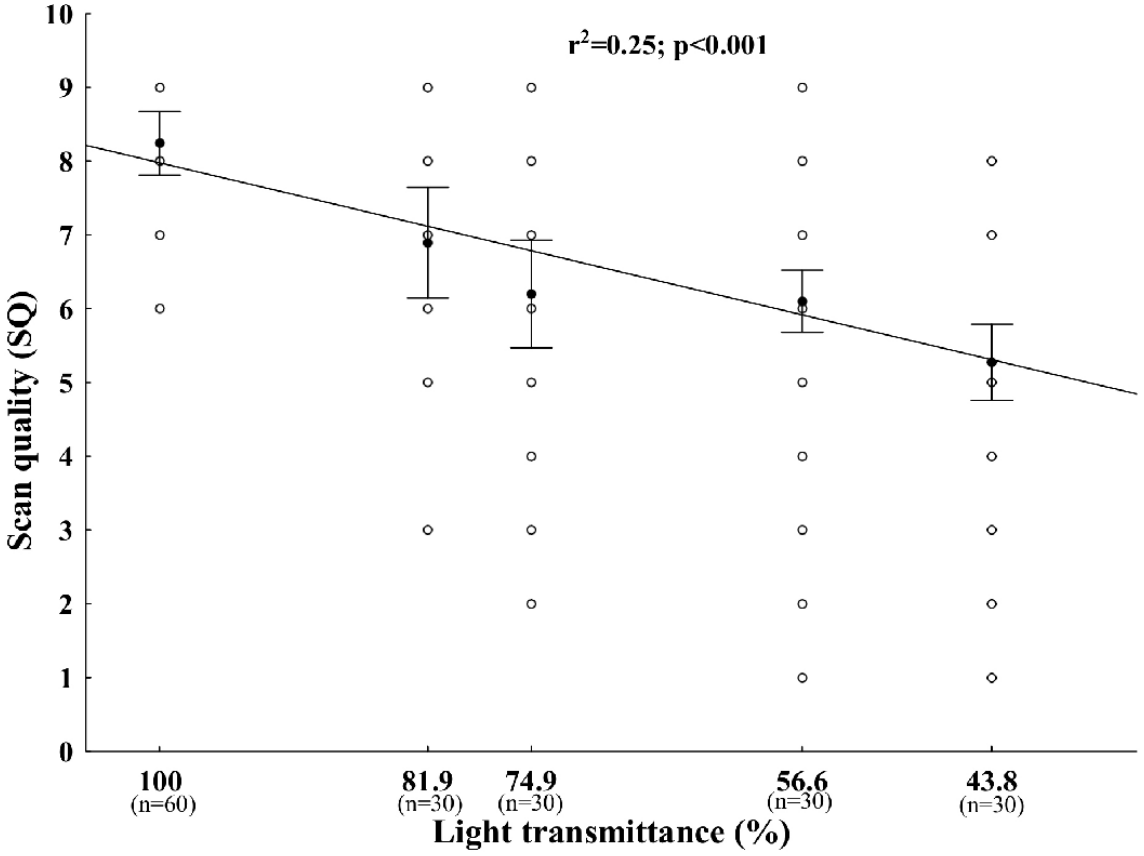

Figure 6. The influence of decreasing light transmittance on corresponding scan quality (SQ). Note: Bars represent the mean ± 95% confidence interval of the mean. Own representation, published in (78).

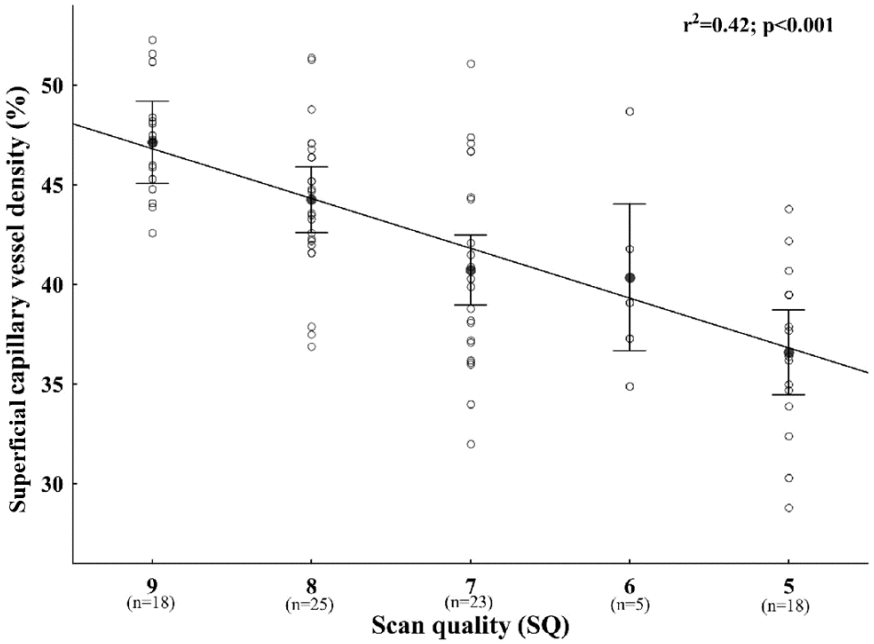

Figure 7. The impact of OCTA scan quality on superficial retinal capillary vessel density (VD) measurements. Note: Bars represent the mean ± 95% confidence interval of the mean. Own representation, published in (78).

To facilitate comparisons of scans acquired with varying image quality, we calculated the average changes in OCTA parameters when SQ values differed by one unit. Table 2 presents the uniform correction factors for the different OCTA parameters, adjusted for scan quality between 5 and 10. These correction factors were significant for macular and peripapillary VD measurements, with the exception of peripapillary small VD (Table 2). Conversely, a one-unit change in image quality did not affect NF, FAZ area, or thickness data (Table 2).

Table 2. The effect of a one-unit change in scan quality on OCTA parameters within the recommended range of image quality (SQ: 5–10). VDAV: vessel density all vessels, VDSV: vessel density small vessels

Scan type		Mean	SE	95% CI	*p*
OCTA macula	**VD superficial layer (%)**	**3.64**	**0.99**	**1.69 – 5.61**	**<0.001**
	VD deep layer (%)	**3.05**	**1.47**	**0.15 – 5.94**	**0.03**
	Non flow area (mm^2)	0.03	0.04	-0.06 – 0.13	0.51
	FAZ area (mm^2)	0.03	0.04	-0.06 – 0.11	0.53
OCTA optic nerve head	**VDAV whole image (%)**	**3.02**	**1.19**	**0.69 – 5.35**	**0.01**
	VDSV whole image (%)	**2.27**	**1.17**	**0.03 – 4.56**	**0.04**
	VDAV peripapillary (%)	**3.92**	**1.67**	**0.64 – 7.19**	**0.01**
	VDSV peripapillary (%)	2.40	1.51	-0.57 – 5.36	0.11
OCT	**Average macular thickness (µm)**	0.68	2.23	-3.69 – 5.06	0.76
	Foveal thickness (µm)	3.98	4.38	-4.59 – 12.56	0.36
	RNFL thickness (µm)	9.03	10.44	-11.43 – 29.50	0.39

4.2. Impact of systemic factors on OCTA measurements in patients with carotid stenosis

4.2.1. Patients' characteristics

A total of 112 eyes of 56 patients (26 male and 30 female, mean age: 69.89 ± 7.07 years) were included in the study. The mean degree of stenosis was 79.80 ± 8.96% (non-compromised CoW 80.38 ± 5.94%; compromised CoW 79.14 ± 9.66%; $p = 0.62$). The incidence of near occlusion (90–99% degree of stenosis) and significant stenosis (70–89% degree of stenosis) did not differ significantly. The baseline characteristics of the study group are presented in Table 3.

Table 3. Baseline characteristics of the study group

	Mean ± SD	Min - Max
Age (years)	69.89 ± 7.07	53 – 84
Gender (F/M)	22 / 34	-
Carotid stenosis (%)	79.80 ± 8.96	50 – 99
Hypertension (Y/N)	52 / 4	-
Diabetes (Y/N)	21 / 35	-
Acetyl salicylic acid use (Y/N)	33 / 23	-
Clopidogrel use (Y/N)	21 / 35	-
Statin use (Y/N)	33 / 23	-
BMI	28.48 ± 5.64	18.31 – 42.24
Creatinin (umol/l)	92.43 ± 40.31	46 – 257
eGFR (ml/min/1.73 m^2)	69.82 ± 18.61	22 – 90
Cholesterol (mmol/l)	4.57 ± 1.49	2.20 – 9.70
HDL (mmol/l)	1.16 ± 0.26	0.61 – 2.08
LDL (mmol/l)	2.65 ± 1.07	0.81 – 6.30
Triglyceride (mmol/l)	1.98 ± 1.14	0.60 – 6.88

4.2.2.OCT angiographic measurements

The SQ values ranged from 6 to 10, with an overall mean SQ of 7.45 ± 1.01. There was no statistically significant difference between the SQ values of the ipsilateral and contralateral side (7.49 ± 0.99 vs. 7.41 ± 1.01; $p = 0.12$). Scan quality was included as a confounder in all statistical calculations, as it was found to be a significant predictor of superficial capillary density (2.52%; 95% CI: 2.33–2.73%; $p < 0.001$). Significant predictors of macular vessel density in both bivariable and multivariable models are summarized in Table 4. We identified estimated glomerular filtration rate (eGFR), statin use, hypertension, degree of carotid occlusion, and carotid surgery as significant predictors of superficial macular vessel density. Even after adjusting for the effect of scan quality, none of the other systemic factors were significant predictors of retinal vessel density. Even after controlling for the negative effect of hypertension, carotid occlusion,

and lower eGFR in these patients, statin use had a significant positive effect on retinal microcirculatory parameters (Table 4). The relative effect of significant predictors is summarized in Figure 8.

Table 4. Significant predictors of macular vessel density in patients with CAS. Note: Bivariable models included scan quality and one predictor. Multivariable models included all listed predictors.

	Superficial capillary layer					
	Bivariable analysis			**Multivariable analysis**		
	Beta	**95% CI**	***p***	**Beta**	**95% CI**	***p***
Scan quality (unit)	2.52	2.33 – 2.73	<0.001	2.16	1.96 – 2.37	<0.001
Carotid stenosis (10%)	-0.11	-0.05 – -0.17	0.001	-0.10	-0.04 - -0.16	0.001
Hypertension (Y/N)	-1.56	-0.77 – -2.34	<0.001	-1.46	-0.68 - -2.23	<0.001
eGFR (10 units)	0.34	0.23 – 0.45	<0.001	0.35	0.24 – 0.46	<0.001
Statin use (Y/N)	0.95	0.53 – 1.37	<0.001	1.02	0.60 – 1.44	<0.001
Surgery	0.54	0.12 – 0.96	0.01	0.55	0.14 – 0.95	0.01
Age (years)	-0.12	-0.09 – -0.15	<0.001	-0.08	-0.06 - -0.12	<0.001

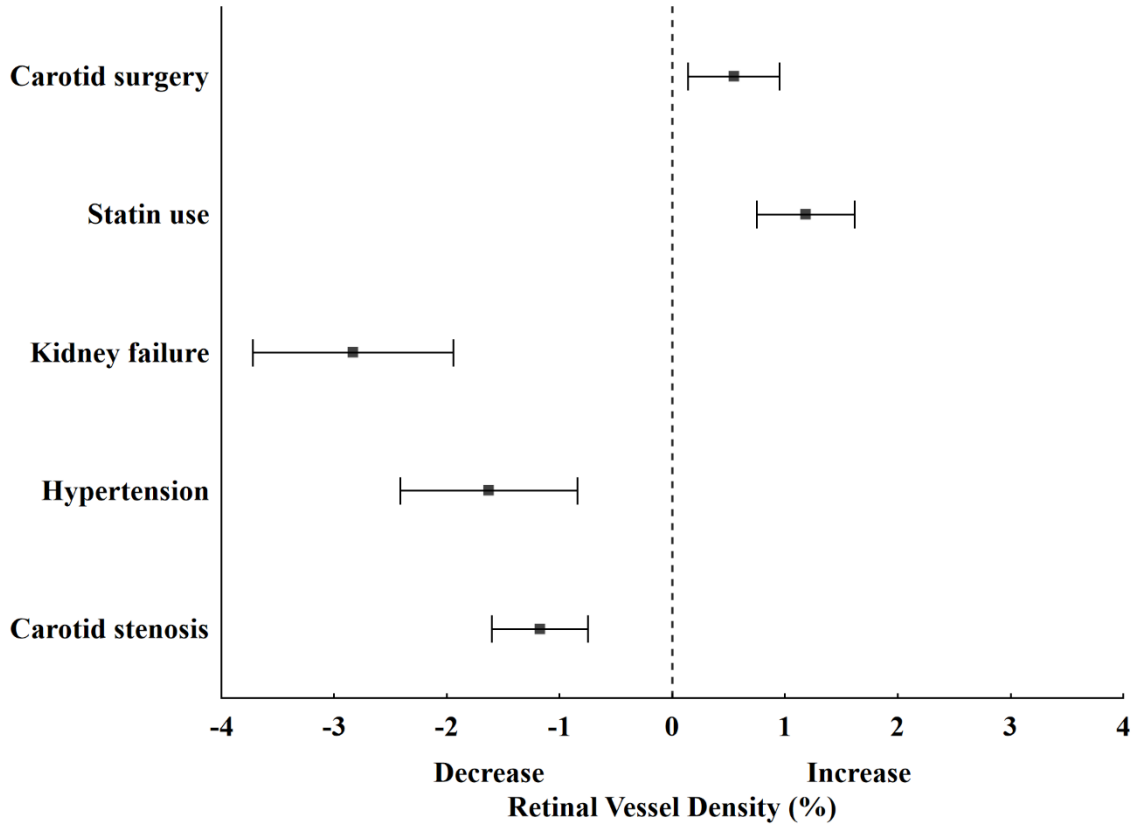

Figure 8. The forest plot illustrates the effect estimates of systemic predictors and carotid surgery on superficial retinal vessel density, adjusted for scan quality. Own representation, published in (79).

An example of macular vessel density in both eyes of a patient with significant left carotid artery stenosis is shown in Figure 9.

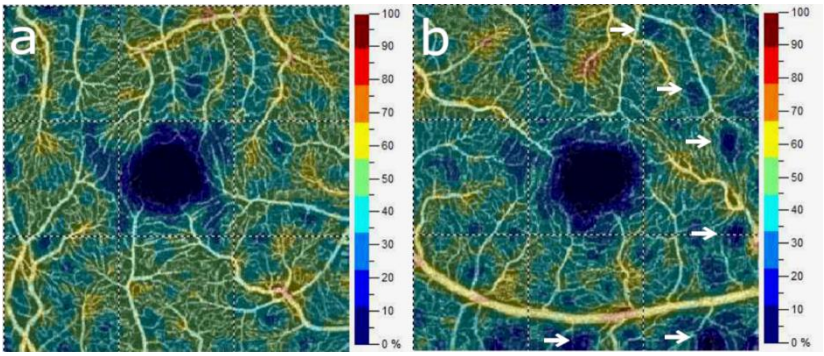

Figure 9. Color-coded representations of macular vessel density (VD) in both eyes of a patient with left unilateral carotid artery stenosis exhibit maintained retinal blood flow (VD: 44.7%) in the contralateral right eye (a), whereas the ipsilateral left eye (b) displays areas of non-perfusion (indicated by arrows) and reduced overall perfusion (VD: 41.9%). Own image, published in (79).

4.2.3. CoW analysis and correlation to OCTA measurements

Patients underwent preoperative CTA of the extra- as well as intracranial cerebral circulation and pre- and postoperative OCT. Patients were classified into two groups based on the status of their Circle of Willis: (I) compromised CoW, containing at least one non-visualized segment, and (II) non-compromised CoW, comprising hypoplastic and normal segments. Figure 10 illustrates examples of the CoW subgroups. Table 5 demonstrates the prevalence of hypoplastic, normal, and non-visualized segments in patients' CoW morphologies. The incidence of different CoW morphologies was similar among patients with ipsilateral 70–89% stenosis and those with subocclusive (90–99%) stenosis, with the rate of non-compromised CoW being 25% and 16.7%, respectively. After adjusting for image quality in a multivariable analysis, the status of the CoW was found to be a significant influencing factor on superficial macular vessel density (0.87; CI: 0.26–1.50; p = 0.005) with vessel density being significantly lower in the compromised CoW group. Further detailed characteristics of the patients are presented in Table 6.

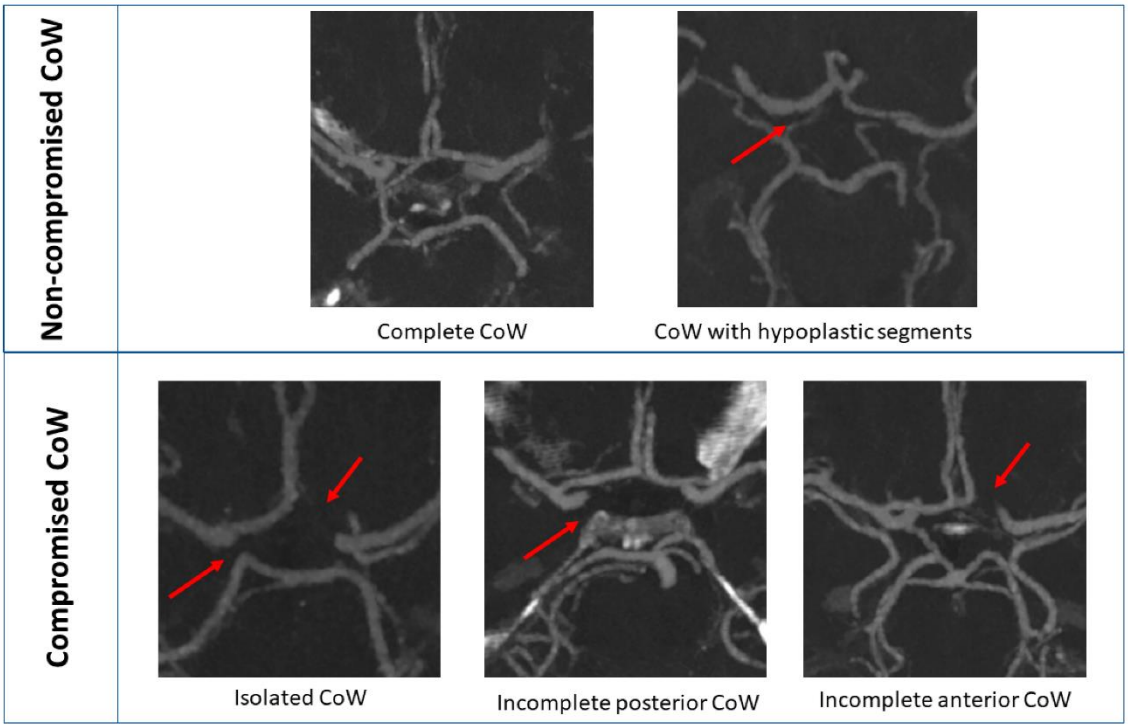

Figure 10. The maximum intensity projection of the CTA provides an overview of the compromised and non-compromised CoW. The red arrow indicates the hypoplastic or non-visualized segments. Image of our working group, published in (80).

Table 5. Incidence of normal, hypoplastic, and non-visualized segments of CoW morphologies. ACoA: anterior communicating artery, A1: anterior cerebral artery, PCoA: posterior communicating artery, P1: posterior cerebral artery, CoW: circle of Willis.

All (n = 56)	Normal segment	Hypoplastic segment	Non-visualized segment
ACoA (N)	94.6% (53)	1.7% (1)	3.6% (2)
A1 (Nx2)	91.9% (103)	4.5% (5)	3.6% (4)
PCoA (NX2)	44.6% (25)	19.6% (11)	35.7% (20)
P1 (Nx2)	86.6% (97)	8.0% (9)	5.4% (6)
Anterior CoW semicircle	64.3% (36)	25.0% (14)	10.7% (6)
Posterior CoW semicircle	37.5% (21)	28.6% (16)	37.5% (21)

Table 6. Clinical characteristics and CoW morphology of study subjects, including those with ipsilateral ICA stenosis in the 70–89% range and those in the subocclusive 90–99% range.

	All patients	**70-89% ICA stenosis**	**90-99% ICA stenosis**	***p***
Number of patients n (%)	56	44	12	
Significant contralateral ICA stenosis/occlusion n (%)	10 (17.9%)	9 (20.5%)	1 (8.3%)	0.67
Symptomatic ICA stenosis n (%)	4 (7.1%)	3 (6.7%)	1 (8.3%)	1.00
Circle of Willis morphology subgroups				
Non-compromised	13 (23.2%)	11 (25%)	2 (16.7%)	0.71
Compromised	43 (76.8%)	33 (75%)	10 (83.3%)	

5. Discussion

The present findings indicate that OCTA parameters exhibit significant differences between scans with lower image quality compared to those with higher quality despite all acquired images having acceptable scan quality. The clinical relevance of these findings is that in longitudinal patient follow-ups, the intra-individual fluctuations in OCTA data are frequent and non-negligible. Therefore, these fluctuations must be taken into account when interpreting OCTA data.

There are several potential reasons for attenuated image quality, including media opacity, floaters, blinking artifacts, eye saccades, and operator error during image acquisition. Such factors can lead to increased measurement variability. Although it is well established that the quality of OCTAs is of critical importance for accurate medical diagnosis, the effect of image quality on quantitative OCTA parameters remains to be fully identified. A recent study examined the relationship between Signal Strength Index (SSI) and macular superficial vessel density (SVD) measurements on two OCTA systems, in which signal strength reduction was generated by either neutral density filters or defocus (72). However, the aforementioned study did not address the impact of image quality on subsequent OCTA parameters and the necessity for correction factors in comparative analysis. Other studies have demonstrated that media opacities cause signal loss (67), and lower image quality is associated with increased artifact frequency and lower repeatability in healthy volunteers (74). Cataracts can notably impact quantitative measurements of vasculature, even in high-quality images acquired through swept-source OCTA (73). Another recent investigation highlighted that posterior subcapsular cataracts may decrease peripapillary vessel density, potentially misinterpreting glaucoma progression (75). Additionally, research indicates that images with lower signal-to-noise ratios are linked to less precise segmentation of retinal layers, resulting in falsely reduced thickness measurements (81-84). While previous studies have addressed the repeatability of OCTA measurements across scans with varying image quality (reflecting statistical error), there remains a dearth of data on the deterministic relationship between image quality and OCTA parameters (representing systematic error). Inaccuracies in these measurements could lead clinicians to misinterpret changes in OCTA parameters

resulting from signal intensity loss as genuine changes on follow-up scans. This consideration is particularly crucial in monitoring and managing diseases with slow progression, such as glaucoma. In the elderly population, cataracts are a common cause of media opacity that can affect OCT image quality and measurements (81, 85). As cataracts and retinal vascular diseases frequently coexist in the same eye, the progressive clouding of the lens can act as a confounding factor in the follow-up of patients using OCTA, similar to retinal thickness measurements (86-94). This study sought to examine the correlation between several ocular parameters, including SQ, CRT, RNFL thickness, macular VD, peripapillary VD, NF area, and FAZ area, with the aim of determining if SQ affects OCTA measurements above the recommended threshold. The results of this investigation align with those previously reported by Yu et al., which found that superficial VD measurements are significantly affected by OCT signal strength (72). Contrary to prior research that indicated a positive correlation between image quality and peripapillary RNFL thickness (95), no such correlation was found in this study. Potential explanations for this discrepancy include the inclusion of images with scan quality below the recommended threshold (81, 96) in prior studies and the use of different metrics for image quality. Previous studies have utilized the signal-to-noise ratio (SNR) to describe image quality. In contrast, the present study employed the SQ index, which also considers artifacts from eye motion and defocus.

In our study, the immediate change in image quality was achieved by placing density filters in front of the eye, eliminating the potential for alteration in retinal blood flow. This approach differed from other studies that evaluated the effect of cataract extraction on OCTA measurements. To further support our findings, we also performed OCTA measurements with a glass plate in front of the eye, similar in thickness to the absorptive filters. This assumption was confirmed by the results, as image acquisition using a clear piece of glass did not result in a significant change in image quality. As the true values of OCTA parameters should be constant during consecutive imaging of the same eye over such a short time, our findings represent only the effect of SQ on OCTA metrics. In other words, by taking OCTA images with and without an absorptive filter shortly one after the other, it is exclusively the difference in light attenuation that can affect the scan quality (95). Therefore, the association between SQ and superficial macular and peripapillary VD is supposed to be due to the artifactual bias of the SSADA algorithm of the

AngioAnalytics software. In conclusion, the present study builds upon previous research by emphasizing the importance of recognizing that OCTA parameters calculated with different algorithms are not interchangeable (97-101). Thus, longitudinal monitoring of these measurements should be conducted using the same instrument (102) and, as demonstrated by the results of this study, should account for fluctuations in image quality.

In the second part of our study, we investigated the potential of OCT angiography to detect retinal circulatory disturbances in cases of severe carotid stenosis with typically reduced intracranial circulation. Regarding the effects of systemic factors on OCTA measurements in patients with severe carotid artery stenosis, we reported that the use of statins significantly improved retinal microcirculatory parameters. In contrast, several others, such as decreased eGFR, hypertension, and carotid occlusion, had a significant negative effect. Confirming previous results, image quality had a statistically significant impact on vessel density and should be considered when analyzing retinal blood flow using OCT angiography. Interestingly, neither diabetes, clopidogrel, or acetylsalicylic acid use, BMI, serum lipid level, nor platelet count showed a significant effect on ocular blood flow. One explanation for this observation is that the simultaneous analysis of strong predictors such as hypertension or statin use reduces the strength of the association between these risk factors and retinal blood flow. The findings of this study have several clinical implications, as OCTA technology allows for the investigation of retinal microcirculation before vascular alterations are visible on fundus examination. Consequently, OCTA could serve as a valuable biomarker for the early diagnosis of retinal vascular diseases, glaucoma (103, 104), Alzheimer's disease (105), and other conditions.

Hypertension impacts microcirculation primarily through arteriolar remodeling and capillary rarefaction. Arteriolar remodeling involves inward eutrophic changes due to increased wall stress, mediated by vasoconstriction and oxidative stress pathways (106, 107). Capillary rarefaction, first observed by Ruedemann in the conjunctiva (108), results from vascular destruction outpacing angiogenesis. The development of capillary rarefaction is thought to result from an imbalance between increased vascular destruction and insufficient angiogenesis (106). Video capillaroscopy shows 10–20% lower capillary density in hypertensive patients compared to normotensive controls (109). Interestingly,

reduced capillary density was also found in borderline hypertensive patients and normotensive offsprings of hypertensive parents, raising the possibility that capillary rarefaction is not a direct cause of hypertension but that other microcirculatory defects lead to the development of hypertension (110-112). These changes have also been observed in the cerebral circulation. Studies revealed altered autoregulation and vessel structure in hypertensive patients (113-116). Chronic hypertension is associated with retinal microvascular changes, including increased intercapillary distance, decreased capillary area, and reduced retinal capillary flow, as demonstrated by Doppler flowmetry (22, 117). OCTA also shows reduced vessel density in the superficial and deep retinal capillary plexus and an enlarged foveal avascular zone in hypertensive patients compared to normotensive controls (118, 119). However, none of these studies controlled for scan quality, which may affect comparisons and measurements of retinal blood flow fluctuations in these patients.

Previously, population-based studies linked lower eGFR with impaired cerebral blood flow (120), and MRI scans associated renal function with subclinical markers of cerebral microvascular disease (121). OCT angiography revealed decreased vessel density in the superficial vascular complex, correlating with reduced eGFR in diabetic patients (122). However, this is the first study to describe the significant association between eGFR and retinal blood flow in patients with CAS, independent of diabetes. While microvascular changes in diabetic retinopathy are well-documented, this study highlights broader microvascular implications related to renal function. However, it's still controversial whether microcirculatory changes are a cause or an effect of reduced renal function. The kidney's unique glomerular capillary bed structure predisposes it to ischemia, but evidence suggests renal dysfunction may also contribute to microvascular impairment. Studies link coronary microvascular dysfunction with renal disease (123-126), and impaired cerebral autoregulation correlates with reduced renal function in acute ischemic stroke patients (127). In mice, they found a correlation between progressive renal function loss and microvascular rarefaction, indicating kidney disease may initiate microcirculatory defects independently of atherosclerosis (128).

This study has demonstrated that statin use benefits retinal blood flow. Statins are considered the first-line treatment in most cases of CAS, as they have been proven to slow

down or even partially reverse atherosclerosis. Furthermore, statins appear to improve peripheral endothelial function and decrease carotid intima-media thickness (129). Besides lowering LDL-cholesterol, statins have anti-inflammatory, anticoagulant, and anti-thrombotic properties (130). Though limited data exist on their effect on peripheral microvasculature, some studies confirm benefits for microcirculation, including improved erythrocyte deformation (131). and cutaneous blood flow in hypertriglyceridemia (132). Statins also elevate cerebral blood flow in animal models through NO-dependent and NO-independent mechanisms (133-135), while human studies show protective effects primarily associated with vasoreactivity (136, 137). Recent research links statins to improved capillary rarefaction in the brain and skeletal muscle (138). Haak et al. found significant microcirculation improvements with fluvastatin using nailfold capillaroscopy and laser Doppler perfusion monitoring (139). Our results suggest that OCTA can be a valuable tool for further understanding statin-associated microcirculation changes, potentially corroborating previous findings.

Previous studies have examined ophthalmological changes in CAS patients, comparing both morphological and functional parameters with healthy controls or between the eyes of unilateral CAS patients. Havelius et al. compared dark adaptation levels between unilateral CAS patients and healthy controls, finding significantly lower levels in the patient group without inter-eye differences (140). In a further study, functional changes were assessed in conjunction with blood flow alterations. Ocular pneumoplethysmography was employed to evaluate ophthalmic artery systolic pressure, while retinal function was tested by multifocal electroretinography (mfERG) in patients with unilateral stenosis and no manifest ocular complication. The results demonstrated a significantly delayed and reduced electroretinographic response in the ipsilateral eye. Furthermore, a positive correlation was observed between the mfERG results and the arterial blood pressure (141). Spectral domain optical coherence tomography (SD-OCT) scans in CAS patients by Sayin et al. showed reduced choroidal thickness compared to controls, with no significant differences in RNFL, macular, and GCC thicknesses (142). Wang et al. correlated RNFL thinning with asymptomatic CAS using SD-OCT (143). Other studies reported RNFL and macular thinning in CAS patients compared to healthy controls (144), while Hessler et al. found no morphological or functional differences in retinal parameters between CAS patients and controls (145).

The association between the prevalence of carotid stenosis and other systemic and ophthalmic diseases has been widely investigated. Several studies have examined its connection with diabetes. Ali et al. and Hoke et al. found a significant correlation between asymptomatic carotid stenosis and diabetes mellitus (146, 147). Another study analyzed demographic data from patients who underwent carotid duplex sonography due to ocular indications such as amaurosis fugax or ocular ischemic syndrome. They found that carotid stenosis was most frequent in patients presenting with retinal artery occlusion, ocular ischemic syndrome, anterior ischemic optic neuropathy, diabetic retinopathy, neovascular glaucoma, and central retinal vein occlusion. Among the demographic factors, they reported only diabetes to be predictive of carotid stenosis. Other researchers performed carotid artery ultrasound on patients with microvascular retinopathy and found retinal artery occlusion and diabetic retinopathy to be significantly associated with substantial carotid artery disease (148). Further studies have investigated the prevalence of carotid stenosis in patients with glaucoma. Marmion et al. reported significant levels of internal carotid artery disease in patients with primary open-angle glaucoma (149). Another research group concluded that carotid artery stenosis is an independent risk factor for developing open-angle glaucoma (150).

We also found that carotid surgery significantly improved vessel density of the superficial capillary plexus both ipsi- and contralaterally, independent of systemic factors. As a form of tertiary prevention, carotid artery reconstruction is the primary and most effective intervention for patients following a neurological event. In clinical guidelines, a level IIa recommendation for asymptomatic patients with significant carotid artery stenosis suggests open carotid reconstruction if assessments such as cerebrovascular reserve capacity via TCD, along with plaque progression and morphology through ultrasound or MR, indicate an elevated stroke risk (41, 151). Consequently, the restoration of cerebral blood flow can alleviate ischemic symptoms and prevent further brain damage (152). There is currently no consensus on the indication for carotid reconstruction to improve cerebral blood flow. However, studies suggest that increased retinal blood flow post-CEA correlates with improved visual outcomes and reduced retinal ischemia (153, 154). Enhanced cerebral blood flow after carotid artery reconstruction may also improve cognitive function, suggesting potential benefits for asymptomatic patients (152).

Improvement in cerebrovascular hemodynamics can be observed already in the early postoperative period (155).

Other study groups have examined the effect of carotid endarterectomy on ocular parameters. Yan et al. examined subjective and objective visual functions, including visual acuity, visually evoked potential, electroretinographic parameters, and static and kinetic visual field. The results demonstrated a significant improvement in these areas. Conversely, no change was observed in RNFL thickness (156). Nevertheless, other studies have identified a significant reduction in peripapillary RNFL thickness following surgery (157). Another study reported a significant increase in choroidal thickness in patients with 50–70% stenosis, as evaluated by enhanced depth imaging optical coherence tomography (EDI-OCT) images (158). In a recent study, Lahme et al. measured retinal flow density values in OCTA images and observed a reduced flow density in patients with CAS compared to healthy controls. However, they were unable to identify any difference between the retinal circulation of the ipsilateral and contralateral eyes. After carotid endarterectomy, significant improvement in the radial peripapillary capillary network (RPC) was also identified in the same study; however, no significant change was observed in the superficial or deep layers of the macular area (153). Lee et al. conducted an OCTA examination to evaluate the impact of the surgical procedure for CAS on retinal microcirculation. They observed a significant increase in vessel density within the macular deep vessel complex in both eyes. In the contralateral eye, the vessel density was also observed to have improved in the superficial layer (154).

The CoW structure is sourced from the afferent arteries of the two ICAs and the basilar artery. In imaging studies, the complete morphology of the entire CoW was reported in 27–90% of individuals with no history of cerebrovascular disease and 18–55% of individuals with diagnosed cerebrovascular disease (77, 159). The prevalence of complete CoW is higher in women than in men across all age groups, although it declines with age in both sexes (160). The incidence of CoW variations in our patient group remains consistent with previously published data. The lack of difference in sex distribution in our cohort is likely attributable to the smaller sample size. The incidence of CoW variation in the 70–89% and 90–99% stenosis groups was similar.

The collateral capacity of a vessel appears to be determined by luminal caliber based on the findings of a transcranial Doppler (TCD) study (161). The threshold diameter for cross-flow through the main collateral arteries was reported to be between 0.4 and 0.6 mm in the CoW in the aforementioned study that utilized TCD and postmortem CoW morphology analysis. Normal and hypoplastic segments were defined with a threshold of 0.8 mm, based on a previously published research on imaging the CoW (77). Given the number of enrolled patients and the variable occurrence of the different segment variations, further subgroup analysis involving the separation of hypoplastic and normal CoW segmentations was not possible. A study including 38 patients with unilateral ICA occlusion demonstrated that the pattern of collateral supply significantly impacts the hemodynamic status (162). The results indicated that collateral flow via the ACoA is indicative of a preserved hemodynamic status, whereas the absence of collateral flow via the CoW or flow via only the PCoA is indicative of a deteriorated cerebral hemodynamic perfusion. The best-preserved hemodynamics were reported when both the anterior and posterior circles of the CoW were complete (163). The number of compromised anterior circles of the CoW was low (n = 6) in our study, rendering further statistical analysis impractical. Consequently, this hypothesis cannot be tested in our cohort. It has previously been reported that carotid endarterectomy increases cerebral blood flow only if the degree of stenosis is greater than 90% (164). In our study, the subgroup of patients with 70–90% stenosis and 90–99% subocclusive stenosis demonstrated no statistically significant difference between the compromised and non-compromised CoW morphology.

Collateral circulation is critical in cerebrovascular disease but has often been underrecognized. While the internal carotid artery is the primary vessel for cerebral blood flow compensation, the significant contributions of the external carotid artery and vertebral artery emphasize their importance (165). Arterial flow reduction due to extracranial or intracranial carotid artery stenotic disease is known to promote collateral recruitment in chronic cerebral hypoperfusion. However, the relationship between these collaterals, cerebral blood flow, and clinical symptomatology remains unclear. It is thought that the reinforcement from the collaterals likely depends on several compensatory hemodynamic, metabolic, and neural mechanisms. However, the changes to cerebrovascular intervention resulting from these mechanisms are unknown.

Diagnostic imaging of collaterals is limited to techniques such as TCD, CTA, MRA, and conventional angiography, which have their limitations (166). OCTA may emerge as a more sensitive and clinically easier-to-apply diagnostic tool to measure ophthalmic collateral flow. The recruitment of collaterals in the CoW and the clinical manifestations of carotid artery disease are highly variable. Due to the high variability in anatomic variations of the CoW and the contralateral or intracranial carotid and vertebral arteries, the potential number of variations is considerable. In most cases, the contralateral ICA secures the bilateral anterior cerebral artery (ACA) territory, not just the middle cerebral artery (MCA) on the ipsilateral side of the stenosis (167). As a result of collateral recruitment, a compromised blood flow rate in the MCA is not necessarily related to the degree of carotid stenosis.

A number of publications have described the results of retinal ischemic injury resulting from the occlusion of the common carotid artery in animal models, with the confirmation of retinal ischemia achieved by blocking the collateral flow from the CoW (168, 169). Previous intraoperative measurements indicated that monitoring the orbital vessels can confirm the patency of the Circle of Willis. These findings suggest that retinal blood flow may serve as an "acoustic window" into intracranial blood flow during cardiac surgery (170). In this study, patients with non-compromised CoW exhibited superior ocular blood flow compared to subjects with compromised CoW. The marked enhancement in retinal capillary perfusion in both eyes after carotid endarterectomy indicates a remodeling of intraorbital blood flow following revascularization. These results suggest that patients with non-compromised CoW may experience enhanced benefits, including improved retinal and potentially cerebral function. This evidence could be a valuable consideration in determining indications for carotid reconstruction.

It is evident that this study is not without limitations. The acquired data was obtained using a specific type of device in both studies, which may influence the generalizability of our results. Nevertheless, the findings of our first investigation indicate a clear correlation between OCT image quality and measurement outcomes. Further studies should be conducted with larger cohorts of patients to validate the correction factors and the associated P-values. While SQ-adjusted OCTA values are associated with improved comparability of scans, whether an SQ correction model would enhance our ability to

monitor the progression of diseases affecting retinal microcirculation remains to be examined. However, any advancement that improves the ability to detect true changes in retinal microvasculature over time is of great value. Future studies are required to assess the role of compensation for SQ on OCTA metrics in the clinical setting. The results of the second part of this study demonstrate a clear association between specific systemic risk factors and retinal blood flow in this patient population. As with the first study, further research involving larger patient cohorts is needed to confirm these associations and explore their connection to intracranial blood flow. Finally, while image quality-adjusted OCTA values facilitate improved comparability of scans, it remains to be examined whether the detection of changes in retinal microcirculation would enhance our ability to assess intracranial blood flow in patients with carotid occlusion. However, any advancement that enhances the capacity to identify true alterations in intracranial blood flow over time is beneficial, with future studies likely to assist in evaluating the role of OCTA metrics within the clinical setting. In conclusion, implementing OCTA imaging in the diagnostic armamentarium might result in an increased accuracy of the assessment of the progression and treatment of these patients.

6. Conclusions

Our results confirmed that scan quality significantly impacts the measured OCTA parameters. This effect persists even when the image quality is above the acceptable threshold. This finding may be particularly important for the long-term monitoring of certain diseases. We were also able to quantify the effect of a one-unit change in scan quality on different OCTA parameters. Our study underscores the importance of considering systematic changes in image quality when evaluating OCTA parameters over time in clinical practice. Maintaining consistent scan quality or applying appropriate correction factors is recommended for accurate disease progression assessment. This research contributes to the translational relevance of OCTA by emphasizing the need for standardized image quality measures to ensure reliable longitudinal analysis of OCTA parameters.

OCTA has proven to be a valuable tool for assessing microcirculation in patients with carotid stenosis. Our findings clearly indicate that a systematic relationship exists between specific systemic risk factors and retinal blood flow in this patient population. The factors that have a significant negative effect on retinal blood flow include decreased eGFR, hypertension, and carotid occlusion, while statin use and carotid surgery substantially improve ocular blood flow. Confirming previous results, image quality had a statistically significant impact on vessel density. We found that carotid surgery significantly improved retinal blood flow both ipsi- and contralaterally, independently of systemic factors. Notably, previous studies did not consider the impact of image quality on OCTA parameters or evaluate the influence of systemic factors on retinal blood flow data from two eyes of the same subject, which were addressed in our study.

The CoW serves as the most crucial collateral pathway for maintaining perfusion in the affected vascular territory. The anatomical features of the CoW significantly influence the outcomes of carotid artery stenosis. The ACoA and the PCoA are regarded as the primary collateral pathways in patients with ICA stenosis. In cases where patients have a non-compromised CoW and are candidates for carotid reconstruction, ocular blood flow appears to be better than in those with compromised CoW. The significant improvement in retinal capillary perfusion in both eyes after CEA suggests a reorganization of

intraorbital blood flow following the procedure. To date, no published studies have examined the association between OCTA measurements and CoW anatomy in patients undergoing CEA. Based on our findings, the use of OCTA measurements alongside the assessment of CoW morphology could help in selecting patients who would benefit most from revascularization procedures.

Our results also have significant value for ophthalmic screening. Given that the conditions for which OCTA is most commonly performed (such as diabetes, age-related macular degeneration, or central retinal vein occlusion) affect the elderly population, there is a high likelihood that many of the patients examined may also have asymptomatic carotid artery stenosis. In light of our findings, it is essential to consider not only the image quality of these examinations but also the impact of carotid stenosis on the retinal circulation and to recommend additional screening for CAS if needed.

7. Summary

CAS is one of the primary causes of mortality and permanent disabilities in the Western world. It results from systemic atherosclerotic disease, which affects the majority of the aging population. OCT angiography is a relatively new, non-invasive diagnostic method that has gained popularity due to being fast and easily reproducible. Cerebral and retinal circulation share similar characteristics, making retinal microvasculature a unique model for studying cerebral small vessel disease pathogenesis in vivo.

First, we aimed to investigate the impact of deterministic signal loss on image quality and subsequent OCTA measurements. We used absorptive filters with varying optical densities to simulate controlled signal loss in 30 eyes from 15 healthy subjects. Our results demonstrated a significant correlation between decreased light transmittance and SQ values and the consequent effect on OCTA parameters, particularly macular and peripapillary VD. We found that attenuated image quality was associated with statistically lower VD values. We determined correction factors ranging from 2.27% to 3.97% per one-unit change in SQ for different VD parameters.

We used OCT angiography to assess the impact of systemic risk factors on retinal blood flow in patients with significant carotid artery stenosis. Our findings indicate that systemic factors such as reduced eGFR, hypertension, and carotid occlusion significantly reduce retinal blood flow. Conversely, statin use and carotid surgery notably enhance ocular microcirculation. These results underscore a clear relationship between specific systemic risk factors and retinal blood flow in this patient cohort.

The CoW serves as the primary collateral pathway in patients with CAS. Our third objective was to compare OCTA results with the morphology of the CoW. Patients were categorized into two groups based on CTA findings: compromised CoW and non-compromised CoW (including hypoplastic and normal segments). Our results indicated that VD was significantly higher in patients with non-compromised CoW morphology (by 0.87% 95%CI (0.26–1.50); $p = 0.005$). This suggests that in cases of carotid artery stenosis, patients with non-compromised CoW may benefit from better preserved ocular blood flow, potentially due to remodeling of intra-orbital blood flow.

8. References

1. de Weerd M, Greving JP, Hedblad B, Lorenz MW, Mathiesen EB, O'Leary DH, Rosvall M, Sitzer M, Buskens E, Bots ML. Prevalence of asymptomatic carotid artery stenosis in the general population: an individual participant data meta-analysis. Stroke. 2010;41(6):1294-1297.
2. Mathiesen EB, Joakimsen O, Bønaa KH. Prevalence of and risk factors associated with carotid artery stenosis: the Tromsø Study. Cerebrovasc Dis. 2001;12(1):44-51.
3. de Weerd M, Greving JP, de Jong AW, Buskens E, Bots ML. Prevalence of asymptomatic carotid artery stenosis according to age and sex: systematic review and metaregression analysis. Stroke. 2009;40(4):1105-1113.
4. Romero JR, Beiser A, Seshadri S, Benjamin EJ, Polak JF, Vasan RS, Au R, DeCarli C, Wolf PA. Carotid artery atherosclerosis, MRI indices of brain ischemia, aging, and cognitive impairment: the Framingham study. Stroke. 2009;40(5):1590-1596.
5. Sander K, Bickel H, Förstl H, Etgen T, Briesenick C, Poppert H, Sander D. Carotid- intima media thickness is independently associated with cognitive decline. The INVADE study. Int J Geriatr Psychiatry. 2010;25(4):389-394.
6. O'Leary DH, Polak JF, Kronmal RA, Kittner SJ, Bond MG, Wolfson SK Jr, Bommer W, Price TR, Gardin JM, Savage PJ. Distribution and correlates of sonographically detected carotid artery disease in the Cardiovascular Health Study. The CHS Collaborative Research Group. Stroke. 1992;23(12):1752-1760.
7. Sztriha LK, Nemeth D, Sefcsik T, Vecsei L. Carotid stenosis and the cognitive function. J Neurol Sci. 2009;283(1-2):36-40.
8. Cheng HL, Lin CJ, Soong BW, Wang PN, Chang FC, Wu YT, Chou KH, Lin CP, Tu PC, Lee IH. Impairments in cognitive function and brain connectivity in severe asymptomatic carotid stenosis. Stroke. 2012;43(10):2567-2573.
9. Matin N, Fisher C, Jackson WF, Dorrance AM. Bilateral common carotid artery stenosis in normotensive rats impairs endothelium-dependent dilation of parenchymal arterioles. Am J Physiol Heart Circ Physiol. 2016;310(10):H1321-H1329.
10. Matin N, Fisher C, Lansdell TA, Hammock BD, Yang J, Jackson WF, Dorrance AM. Soluble epoxide hydrolase inhibition improves cognitive function and parenchymal

artery dilation in a hypertensive model of chronic cerebral hypoperfusion. Microcirculation. 2021;28(1):e12653.

11. Zirak P, Delgado-Mederos R, Dinia L, Martí-Fàbregas J, Durduran T. Microvascular versus macrovascular cerebral vasomotor reactivity in patients with severe internal carotid artery stenosis or occlusion. Acad Radiol. 2014;21(2):168-174.

12. Vasdekis SN, Tsivgoulis G, Athanasiadis D, Andrikopoulou A, Voumvourakis K, Lazaris AM, Stamboulis E. Cerebrovascular reacivity assessment in patients with carotid artery disease: a combined TCD and NIRS study. J Neuroimaging. 2012;22(3):261-265.

13. Takasugi J, Miwa K, Watanabe Y, Okazaki S, Todo K, Sasaki T, Sakaguchi M, Mochizuki H. Cortical Cerebral Microinfarcts on 3T Magnetic Resonance Imaging in Patients With Carotid Artery Stenosis. Stroke. 2019;50(3):639-644.

14. Song J, Kim KH, Jeon P, Kim YW, Kim DI, Park YJ, Park MS, Chung JW, Seo WK, Bang OY, Ay H, Kim GM. White matter hyperintensity determines ischemic stroke severity in symptomatic carotid artery stenosis. Neurol Sci. 2021;42(8):3367-3374.

15. Baradaran H, Mtui EE, Richardson JE, Delgado D, Dunning A, Marshall RS, Sanelli PC, Gupta A. White Matter Diffusion Abnormalities in Carotid Artery Disease: A Systematic Review and Meta-Analysis. J Neuroimaging. 2016;26(5):481-488.

16. Shibata M, Ohtani R, Ihara M, Tomimoto H. White matter lesions and glial activation in a novel mouse model of chronic cerebral hypoperfusion. Stroke. 2004;35(11):2598-2603.

17. Sigfridsson E, Marangoni M, Hardingham GE, Horsburgh K, Fowler JH. Deficiency of Nrf2 exacerbates white matter damage and microglia/macrophage levels in a mouse model of vascular cognitive impairment. J Neuroinflammation. 2020;17(1):367.

18. Longstreth WT, Bernick C, Manolio TA, Bryan N, Jungreis CA, Price TR. Lacunar infarcts defined by magnetic resonance imaging of 3660 elderly people: the Cardiovascular Health Study. Arch Neurol. 1998;55(9):1217-1225.

19. Silvestrini M, Pasqualetti P, Baruffaldi R, Catani S, Tibuzzi F, Altamura C, Bartolini M, Provinciali L, Vernieri F. Markers of lacunar stroke in patients with moderate internal carotid artery stenosis. J Neurol. 2006;253(3):321-327.

20. Ungvari Z, Tarantini S, Kiss T, Wren JD, Giles CB, Griffin CT, Murfee WL, Pacher P, Csiszar A. Endothelial dysfunction and angiogenesis impairment in the ageing vasculature. Nat Rev Cardiol. 2018;15(9):555-565.

21. Tucsek Z, Toth P, Tarantini S, Sosnowska D, Gautam T, Warrington JP, Giles CB, Wren JD, Koller A, Ballabh P, Sonntag WE, Ungvari Z, Csiszar A. Aging exacerbates obesity-induced cerebromicrovascular rarefaction, neurovascular uncoupling, and cognitive decline in mice. J Gerontol A Biol Sci Med Sci. 2014;69(11):1339-1352.

22. Bosch AJ, Harazny JM, Kistner I, Friedrich S, Wojtkiewicz J, Schmieder RE. Retinal capillary rarefaction in patients with untreated mild-moderate hypertension. BMC Cardiovasc Disord. 2017;17(1):300.

23. Chantler PD, Shrader CD, Tabone LE, d'Audiffret AC, Huseynova K, Brooks SD, Branyan KW, Grogg KA, Frisbee JC. Cerebral Cortical Microvascular Rarefaction in Metabolic Syndrome is Dependent on Insulin Resistance and Loss of Nitric Oxide Bioavailability. Microcirculation. 2015;22(6):435-445.

24. Suzuki K, Masawa N, Sakata N, Takatama M. Pathologic evidence of microvascular rarefaction in the brain of renal hypertensive rats. J Stroke Cerebrovasc Dis. 2003;12(1):8-16.

25. Jumar A, Harazny JM, Ott C, Friedrich S, Kistner I, Striepe K, Schmieder RE. Retinal Capillary Rarefaction in Patients with Type 2 Diabetes Mellitus. PLoS One. 2016;11(12):e0162608.

26. Toth P, Tarantini S, Csiszar A, Ungvari Z. Functional vascular contributions to cognitive impairment and dementia: mechanisms and consequences of cerebral autoregulatory dysfunction, endothelial impairment, and neurovascular uncoupling in aging. Am J Physiol Heart Circ Physiol. 2017;312(1):H1-H20.

27. Katusic ZS, Austin SA. Neurovascular Protective Function of Endothelial Nitric Oxide - Recent Advances. Circ J. 2016;80(7):1499-1503.

28. Tarantini S, Valcarcel-Ares MN, Toth P, Yabluchanskiy A, Tucsek Z, Kiss T, Hertelendy P, Kinter M, Ballabh P, Süle Z, Farkas E, Baur JA, Sinclair DA, Csiszar A, Ungvari Z. Nicotinamide mononucleotide (NMN) supplementation rescues cerebromicrovascular endothelial function and neurovascular coupling responses and improves cognitive function in aged mice. Redox Biol. 2019;24:101192.

29. Tarantini S, Valcarcel-Ares NM, Yabluchanskiy A, Fulop GA, Hertelendy P, Gautam T, Farkas E, Perz A, Rabinovitch PS, Sonntag WE, Csiszar A, Ungvari Z. Treatment with the mitochondrial-targeted antioxidant peptide SS-31 rescues

neurovascular coupling responses and cerebrovascular endothelial function and improves cognition in aged mice. Aging Cell. 2018;17(2).

30. Toth P, Tarantini S, Ashpole NM, Tucsek Z, Milne GL, Valcarcel-Ares NM, Menyhart A, Farkas E, Sonntag WE, Csiszar A, Ungvari Z. IGF-1 deficiency impairs neurovascular coupling in mice: implications for cerebromicrovascular aging. Aging Cell. 2015;14(6):1034-1044.

31. Toth P, Tarantini S, Davila A, Valcarcel-Ares MN, Tucsek Z, Varamini B, Ballabh P, Sonntag WE, Baur JA, Csiszar A, Ungvari Z. Purinergic glio-endothelial coupling during neuronal activity: role of P2Y1 receptors and eNOS in functional hyperemia in the mouse somatosensory cortex. Am J Physiol Heart Circ Physiol. 2015;309(11):H1837-H1845.

32. Toth P, Tarantini S, Tucsek Z, Ashpole NM, Sosnowska D, Gautam T, Ballabh P, Koller A, Sonntag WE, Csiszar A, Ungvari Z. Resveratrol treatment rescues neurovascular coupling in aged mice: role of improved cerebromicrovascular endothelial function and downregulation of NADPH oxidase. Am J Physiol Heart Circ Physiol. 2014;306(3):H299-H308.

33. Tarantini S, Tran CHT, Gordon GR, Ungvari Z, Csiszar A. Impaired neurovascular coupling in aging and Alzheimer's disease: Contribution of astrocyte dysfunction and endothelial impairment to cognitive decline. Exp Gerontol. 2017;94:52-58.

34. Chen BR, Kozberg MG, Bouchard MB, Shaik MA, Hillman EM. A critical role for the vascular endothelium in functional neurovascular coupling in the brain. J Am Heart Assoc. 2014;3(3):e000787.

35. Tarantini S, Hertelendy P, Tucsek Z, Valcarcel-Ares MN, Smith N, Menyhart A, Farkas E, Hodges EL, Towner R, Deak F, Sonntag WE, Csiszar A, Ungvari Z, Toth P. Pharmacologically-induced neurovascular uncoupling is associated with cognitive impairment in mice. J Cereb Blood Flow Metab. 2015;35(11):1871-1881.

36. Lamb TD, Collin SP, Pugh EN. Evolution of the vertebrate eye: opsins, photoreceptors, retina and eye cup. Nat Rev Neurosci. 2007;8(12):960-976.

37. Cabrera DeBuc D, Somfai GM, Koller A. Retinal microvascular network alterations: potential biomarkers of cerebrovascular and neural diseases. Am J Physiol Heart Circ Physiol. 2017;312(2):H201-H212.

38. Halliday A, Harrison M, Hayter E, Kong X, Mansfield A, Marro J, Pan H, Peto R, Potter J, Rahimi K, Rau A, Robertson S, Streifler J, Thomas D; Asymptomatic Carotid Surgery Trial (ACST) Collaborative Group. 10-year stroke prevention after successful carotid endarterectomy for asymptomatic stenosis (ACST-1): a multicentre randomised trial. Lancet. 2010;376(9746):1074-1084.

39. Wabnitz AM, Turan TN. Symptomatic Carotid Artery Stenosis: Surgery, Stenting, or Medical Therapy? Curr Treat Options Cardiovasc Med. 2017;19(8):62.

40. Giles MF, Rothwell PM. Risk of stroke early after transient ischaemic attack: a systematic review and meta-analysis. Lancet Neurol. 2007;6(12):1063-1072.

41. Naylor AR, Ricco JB, de Borst GJ, Debus S, de Haro J, Halliday A, Hamilton G, Kakisis J, Kakkos S, Lepidi S, Markus HS, McCabe DJ, Roy J, Sillesen H, van den Berg JC, Vermassen F, Esvs Guidelines Committee, Kolh P, Chakfe N, Hinchliffe RJ, Koncar I, Lindholt JS, Vega de Ceniga M, Verzini F, Esvs Guideline Reviewers, Archie J, Bellmunt S, Chaudhuri A, Koelemay M, Lindahl AK, Padberg F, Venermo M. Editor's Choice - Management of Atherosclerotic Carotid and Vertebral Artery Disease: 2017 Clinical Practice Guidelines of the European Society for Vascular Surgery (ESVS). Eur J Vasc Endovasc Surg. 2018;55(1):3-81.

42. Randomised trial of endarterectomy for recently symptomatic carotid stenosis: final results of the MRC European Carotid Surgery Trial (ECST). Lancet. 1998;351(9113):1379-1387.

43. North American Symptomatic Carotid Endarterectomy Trial Collaborators; Barnett HJM, Taylor DW, Haynes RB, Sackett DL, Peerless SJ, Ferguson GG, Fox AJ, Rankin RN, Hachinski VC, Wiebers DO, Eliasziw M. Beneficial effect of carotid endarterectomy in symptomatic patients with high-grade carotid stenosis. N Engl J Med. 1991;325(7):445-453.

44. Lui EY, Steinman AH, Cobbold RS, Johnston KW. Human factors as a source of error in peak Doppler velocity measurement. J Vasc Surg. 2005;42(5):972-979.

45. Logason K, Bärlin T, Jonsson ML, Boström A, Hårdemark HG, Karacagil S. The importance of Doppler angle of insonation on differentiation between 50-69% and 70-99% carotid artery stenosis. Eur J Vasc Endovasc Surg. 2001;21(4):311-313.

46. István L, Czakó C, Élő Á, Mihály Z, Sótonyi P, Varga A, Ungvári Z, Csiszár A, Yabluchanskiy A, Conley S, Csipő T, Lipecz Á, Kovács I, Nagy ZZ. Imaging retinal

microvascular manifestations of carotid artery disease in older adults: from diagnosis of ocular complications to understanding microvascular contributions to cognitive impairment. Geroscience. 2021;43(4):1703-1723.

47. Naylor R, Rantner B, Ancetti S, de Borst GJ, De Carlo M, Halliday A, Kakkos SK, Markus HS, McCabe DJH, Sillesen H, van den Berg JC, Vega de Ceniga M, Venermo MA, Vermassen FEG, Esvs Guidelines Committee, Antoniou GA, Bastos Goncalves F, Bjorck M, Chakfe N, Coscas R, Dias NV, Dick F, Hinchliffe RJ, Kolh P, Koncar IB, Lindholt JS, Mees BME, Resch TA, Trimarchi S, Tulamo R, Twine CP, Wanhainen A, Document Reviewers, Bellmunt-Montoya S, Bulbulia R, Darling RC 3rd, Eckstein HH, Giannoukas A, Koelemay MJW, Lindström D, Schermerhorn M, Stone DH. Editor's Choice - European Society for Vascular Surgery (ESVS) 2023 Clinical Practice Guidelines on the Management of Atherosclerotic Carotid and Vertebral Artery Disease. Eur J Vasc Endovasc Surg. 2023;65(1):7-111.

48. Brott TG, Hobson RW 2nd, Howard G, Roubin GS, Clark WM, Brooks W, Mackey A, Hill MD, Leimgruber PP, Sheffet AJ, Howard VJ, Moore WS, Voeks JH, Hopkins LN, Cutlip DE, Cohen DJ, Popma JJ, Ferguson RD, Cohen SN, Blackshear JL, Silver FL, Mohr JP, Lal BK, Meschia JF; CREST Investigators. Stenting versus endarterectomy for treatment of carotid-artery stenosis. N Engl J Med. 2010;363(1):11-23.

49. Hill MD, Brooks W, Mackey A, Clark WM, Meschia JF, Morrish WF, Mohr JP, Rhodes JD, Popma JJ, Lal BK, Longbottom ME, Voeks JH, Howard G, Brott TG; CREST Investigators. Stroke after carotid stenting and endarterectomy in the Carotid Revascularization Endarterectomy versus Stenting Trial (CREST). Circulation. 2012;126(25):3054-3061.

50. Kvickström P, Lindblom B, Bergström G, Zetterberg M. Amaurosis fugax: risk factors and prevalence of significant carotid stenosis. Clin Ophthalmol. 2016;10:2165-2170.

51. Furlan AJ, Whisnant JP, Kearns TP. Unilateral visual loss in bright light. An unusual symptom of carotid artery occlusive disease. Arch Neurol. 1979;36(11):675-676.

52. Ros MA, Magargal LE, Uram M. Branch retinal-artery obstruction: a review of 201 eyes. Ann Ophthalmol. 1989;21(3):103-107.

53. Hayreh SS, Kolder HE, Weingeist TA. Central retinal artery occlusion and retinal tolerance time. Ophthalmology. 1980;87(1):75-78.

54. Schrag M, Youn T, Schindler J, Kirshner H, Greer D. Intravenous Fibrinolytic Therapy in Central Retinal Artery Occlusion: A Patient-Level Meta-analysis. JAMA Neurol. 2015;72(10):1148-1154.

55. Mac Grory B, Schrag M, Biousse V, Furie KL, Gerhard-Herman M, Lavin PJ, Sobrin L, Tjoumakaris SI, Weyand CM, Yaghi S; American Heart Association Stroke Council; Council on Arteriosclerosis, Thrombosis and Vascular Biology; Council on Hypertension; and Council on Peripheral Vascular Disease. Management of Central Retinal Artery Occlusion: A Scientific Statement From the American Heart Association. Stroke. 2021;52(6):e282-e294.

56. Klein R, Klein BE, Jensen SC, Moss SE, Meuer SM. Retinal emboli and stroke: the Beaver Dam Eye Study. Arch Ophthalmol. 1999;117(8):1063-1068.

57. Cheung N, Teo K, Zhao W, Wang JJ, Neelam K, Tan NYQ, Mitchell P, Cheng CY, Wong TY. Prevalence and Associations of Retinal Emboli With Ethnicity, Stroke, and Renal Disease in a Multiethnic Asian Population: The Singapore Epidemiology of Eye Disease Study. JAMA Ophthalmol. 2017;135(10):1023-1028.

58. Wong TY, Klein R. Retinal arteriolar emboli: epidemiology and risk of stroke. Curr Opin Ophthalmol. 2002;13(3):142-146.

59. Terelak-Borys B, Skonieczna K, Grabska-Liberek I. Ocular ischemic syndrome - a systematic review. Med Sci Monit. 2012;18(8):RA138-RA144.

60. Matsushima C, Wakabayashi Y, Iwamoto T, Yamauchi Y, Usui M, Iwasaki T. Relationship between retinal vein occlusion and carotid artery lesions. Retina. 2007;27(8):1038-1043.

61. Nicholson L, Talks SJ, Amoaku W, Talks K, Sivaprasad S. Retinal vein occlusion (RVO) guideline: executive summary. Eye (Lond). 2022;36(5):909-912.

62. Patton N, Aslam T, Macgillivray T, Pattie A, Deary IJ, Dhillon B. Retinal vascular image analysis as a potential screening tool for cerebrovascular disease: a rationale based on homology between cerebral and retinal microvasculatures. J Anat. 2005;206(4):319-348.

63. Newman EA. Functional hyperemia and mechanisms of neurovascular coupling in the retinal vasculature. J Cereb Blood Flow Metab. 2013;33(11):1685-1695.

64. Lim M, Sasongko MB, Ikram MK, Lamoureux E, Wang JJ, Wong TY, Cheung CY. Systemic associations of dynamic retinal vessel analysis: a review of current literature. Microcirculation. 2013;20(3):257-268.

65. Lipecz A, Csipo T, Tarantini S, Hand RA, Ngo BN, Conley S, Nemeth G, Tsorbatzoglou A, Courtney DL, Yabluchanska V, Csiszar A, Ungvari ZI, Yabluchanskiy A. Age-related impairment of neurovascular coupling responses: a dynamic vessel analysis (DVA)-based approach to measure decreased flicker light stimulus-induced retinal arteriolar dilation in healthy older adults. Geroscience. 2019;41(3):341-349.

66. Erickson SJ, Hendrix LE, Massaro BM, Harris GJ, Lewandowski MF, Foley WD, Lawson TL. Color Doppler flow imaging of the normal and abnormal orbit. Radiology. 1989;173(2):511-516.

67. Sakata LM, Deleon-Ortega J, Sakata V, Girkin CA. Optical coherence tomography of the retina and optic nerve - a review. Clin Exp Ophthalmol. 2009;37(1):90-99.

68. Huang D, Swanson EA, Lin CP, Schuman JS, Stinson WG, Chang W, Hee MR, Flotte T, Gregory K, Puliafito CA. Optical coherence tomography. Science. 1991;254(5035):1178-1181.

69. Chen TC, Cense B, Pierce MC, Nassif N, Park BH, Yun SH, White BR, Bouma BE, Tearney GJ, de Boer JF. Spectral domain optical coherence tomography: ultra-high speed, ultra-high resolution ophthalmic imaging. Arch Ophthalmol. 2005;123(12):1715-1720.

70. Tan ACS, Tan GS, Denniston AK, Keane PA, Ang M, Milea D, Chakravarthy U, Cheung CMG. An overview of the clinical applications of optical coherence tomography angiography. Eye (Lond). 2018;32(2):262-286.

71. Czakó C, István L, Ecsedy M, Récsán Z, Sándor G, Benyó F, Horváth H, Papp A, Resch M, Borbándy Á, Nagy ZZ, Kovács I. The effect of image quality on the reliability of OCT angiography measurements in patients with diabetes. Int J Retina Vitreous. 2019;5:46.

72. Yu JJ, Camino A, Liu L, Zhang X, Wang J, Gao SS, Jia Y, Huang D. Signal Strength Reduction Effects in OCT Angiography. Ophthalmol Retina. 2019;3(10):835-842.

73. Yu S, Frueh BE, Steinmair D, Ebneter A, Wolf S, Zinkernagel MS, Munk MR. Cataract significantly influences quantitative measurements on swept-source optical coherence tomography angiography imaging. PLoS One. 2018;13(10):e0204501.
74. Al-Sheikh M, Ghasemi Falavarjani K, Akil H, Sadda SR. Impact of image quality on OCT angiography based quantitative measurements. Int J Retina Vitreous. 2017;3:13.
75. Holló G. Influence of Posterior Subcapsular Cataract on Structural OCT and OCT Angiography Vessel Density Measurements in the Peripapillary Retina. J Glaucoma. 2019;28(4):e61-e63.
76. Lei J, Pei C, Wen C, Abdelfattah NS. Repeatability and Reproducibility of Quantification of Superficial Peri-papillary Capillaries by four Different Optical Coherence Tomography Angiography Devices. Sci Rep. 2018;8(1):17866.
77. Varga A, Di Leo G, Banga PV, Csobay-Novák C, Kolossváry M, Maurovich-Horvat P, Hüttl K. Multidetector CT angiography of the Circle of Willis: association of its variants with carotid artery disease and brain ischemia. Eur Radiol. 2019;29(1):46-56.
78. Czakó C, István L, Benyó F, Élő Á, Erdei G, Horváth H, Nagy ZZ, Kovács I. The Impact of Deterministic Signal Loss on OCT Angiography Measurements. Transl Vis Sci Technol. 2020;9(5):10.
79. István L, Czakó C, Benyó F, Élő Á, Mihály Z, Sótonyi P, Varga A, Nagy ZZ, Kovács I. The effect of systemic factors on retinal blood flow in patients with carotid stenosis: an optical coherence tomography angiography study. Geroscience. 2022;44(1):389-401.
80. Mihály Z, István L, Czakó C, Benyó F, Borzsák S, Varga A, Magyar-Stang R, Banga PV, Élő Á, Debreczeni R, Kovács I, Sótonyi P. The Effect of Circle of Willis Morphology on Retinal Blood Flow in Patients with Carotid Stenosis Measured by Optical Coherence Tomography Angiography. J Clin Med. 2023;12(16).
81. Zhang X, Iverson SM, Tan O, Huang D. Effect of Signal Intensity on Measurement of Ganglion Cell Complex and Retinal Nerve Fiber Layer Scans in Fourier-Domain Optical Coherence Tomography. Transl Vis Sci Technol. 2015;4(5):7.
82. Cheung CY, Leung CK, Lin D, Pang CP, Lam DS. Relationship between retinal nerve fiber layer measurement and signal strength in optical coherence tomography. Ophthalmology. 2008;115(8):1347-1351, 51.e13512.

83. Ghahari E, Bowd C, Zangwill LM, Proudfoot J, Hasenstab KA, Hou H, Penteado RC, Manalastas PIC, Moghimi S, Shoji T, Christopher M, Yarmohammadi A, Weinreb RN. Association of Macular and Circumpapillary Microvasculature with Visual Field Sensitivity in Advanced Glaucoma. Am J Ophthalmol. 2019;204:51-61.

84. Moghimi S, Bowd C, Zangwill LM, Penteado RC, Hasenstab K, Hou H, Ghahari E, Manalastas PIC, Proudfoot J, Weinreb RN. Measurement Floors and Dynamic Ranges of OCT and OCT Angiography in Glaucoma. Ophthalmology. 2019;126(7):980-988.

85. Kok PH, van Dijk HW, van den Berg TJ, Verbraak FD. A model for the effect of disturbances in the optical media on the OCT image quality. Invest Ophthalmol Vis Sci. 2009;50(2):787-792.

86. El-Ashry M, Appaswamy S, Deokule S, Pagliarini S. The effect of phacoemulsification cataract surgery on the measurement of retinal nerve fiber layer thickness using optical coherence tomography. Curr Eye Res. 2006;31(5):409-413.

87. Savini G, Zanini M, Barboni P. Influence of pupil size and cataract on retinal nerve fiber layer thickness measurements by Stratus OCT. J Glaucoma. 2006;15(4):336-340.

88. Sánchez-Cano A, Pablo LE, Larrosa JM, Polo V. The effect of phacoemulsification cataract surgery on polarimetry and tomography measurements for glaucoma diagnosis. J Glaucoma. 2010;19(7):468-474.

89. Mwanza JC, Bhorade AM, Sekhon N, McSoley JJ, Yoo SH, Feuer WJ, Budenz DL. Effect of cataract and its removal on signal strength and peripapillary retinal nerve fiber layer optical coherence tomography measurements. J Glaucoma. 2011;20(1):37-43.

90. Liu Y, Samarawickrama C, Pai A, Tariq Y, Mitchell P. Stratus OCT signal strength and reliability of retinal nerve fiber layer measurements. Am J Ophthalmol. 2010;149(3):528-529; author reply 9.

91. Samarawickrama C, Mitchell P. Influence of signal strength on OCT measurements. J Glaucoma. 2009;18(6):499-500; author reply

92. Samarawickrama C, Pai A, Huynh SC, Burlutsky G, Wong TY, Mitchell P. Influence of OCT signal strength on macular, optic nerve head, and retinal nerve fiber layer parameters. Invest Ophthalmol Vis Sci. 2010;51(9):4471-4475.

93. Huang J, Liu X, Wu Z, Sadda S. Image quality affects macular and retinal nerve fiber layer thickness measurements on fourier-domain optical coherence tomography. Ophthalmic Surg Lasers Imaging. 2011;42(3):216-221.

94. Huang Y, Gangaputra S, Lee KE, Narkar AR, Klein R, Klein BE, Meuer SM, Danis RP. Signal quality assessment of retinal optical coherence tomography images. Invest Ophthalmol Vis Sci. 2012;53(4):2133-2141.

95. Kok PH, van den Berg TJ, van Dijk HW, Stehouwer M, van der Meulen IJ, Mourits MP, Verbraak FD. The relationship between the optical density of cataract and its influence on retinal nerve fibre layer thickness measured with spectral domain optical coherence tomography. Acta Ophthalmol. 2013;91(5):418-424.

96. Wu Z, Huang J, Dustin L, Sadda SR. Signal strength is an important determinant of accuracy of nerve fiber layer thickness measurement by optical coherence tomography. J Glaucoma. 2009;18(3):213-216.

97. Shahlaee A, Samara WA, Hsu J, Say EA, Khan MA, Sridhar J, Hong BK, Shields CL, Ho AC. In Vivo Assessment of Macular Vascular Density in Healthy Human Eyes Using Optical Coherence Tomography Angiography. Am J Ophthalmol. 2016;165:39-46.

98. Zhang A, Zhang Q, Chen CL, Wang RK. Methods and algorithms for optical coherence tomography-based angiography: a review and comparison. J Biomed Opt. 2015;20(10):100901.

99. Gao SS, Jia Y, Zhang M, Su JP, Liu G, Hwang TS, Bailey ST, Huang D. Optical Coherence Tomography Angiography. Invest Ophthalmol Vis Sci. 2016;57(9):OCT27-OCT36.

100. Choi J, Kwon J, Shin JW, Lee J, Lee S, Kook MS. Quantitative optical coherence tomography angiography of macular vascular structure and foveal avascular zone in glaucoma. PLoS One. 2017;12(9):e0184948.

101. de Carlo TE, Salz DA, Waheed NK, Baumal CR, Duker JS, Witkin AJ. Visualization of the Retinal Vasculature Using Wide-Field Montage Optical Coherence Tomography Angiography. Ophthalmic Surg Lasers Imaging Retina. 2015;46(6):611-616.

102. Rabiolo A, Gelormini F, Sacconi R, Cicinelli MV, Triolo G, Bettin P, Nouri-Mahdavi K, Bandello F, Querques G. Comparison of methods to quantify macular and peripapillary vessel density in optical coherence tomography angiography. PLoS One. 2018;13(10):e0205773.

103. Akil H, Huang AS, Francis BA, Sadda SR, Chopra V. Retinal vessel density from optical coherence tomography angiography to differentiate early glaucoma, pre-perimetric glaucoma and normal eyes. PLoS One. 2017;12(2):e0170476.

104. Yarmohammadi A, Zangwill LM, Diniz-Filho A, Suh MH, Manalastas PI, Fatehee N, Yousefi S, Belghith A, Saunders LJ, Medeiros FA, Huang D, Weinreb RN. Optical Coherence Tomography Angiography Vessel Density in Healthy, Glaucoma Suspect, and Glaucoma Eyes. Invest Ophthalmol Vis Sci. 2016;57(9):OCT451-OCT459.

105. Querques G, Borrelli E, Sacconi R, De Vitis L, Leocani L, Santangelo R, Magnani G, Comi G, Bandello F. Functional and morphological changes of the retinal vessels in Alzheimer's disease and mild cognitive impairment. Sci Rep. 2019;9(1):63.

106. Feihl F, Liaudet L, Waeber B. The macrocirculation and microcirculation of hypertension. Curr Hypertens Rep. 2009;11(3):182-189.

107. Castorena-Gonzalez JA, Staiculescu MC, Foote C, Martinez-Lemus LA. Mechanisms of the inward remodeling process in resistance vessels: is the actin cytoskeleton involved? Microcirculation. 2014;21(3):219-229.

108. Ruedemann AD. Conjunctival vessels. JAMA. 1933;101(19):1477–1481.

109. Serné EH, Gans RO, ter Maaten JC, Tangelder GJ, Donker AJ, Stehouwer CD. Impaired skin capillary recruitment in essential hypertension is caused by both functional and structural capillary rarefaction. Hypertension. 2001;38(2):238-242.

110. Noon JP, Walker BR, Webb DJ, Shore AC, Holton DW, Edwards HV, Watt GC. Impaired microvascular dilatation and capillary rarefaction in young adults with a predisposition to high blood pressure. J Clin Invest. 1997;99(8):1873-1879.

111. Antonios TF, Rattray FM, Singer DR, Markandu ND, Mortimer PS, MacGregor GA. Rarefaction of skin capillaries in normotensive offspring of individuals with essential hypertension. Heart. 2003;89(2):175-178.

112. Antonios TF, Singer DR, Markandu ND, Mortimer PS, MacGregor GA. Rarefaction of skin capillaries in borderline essential hypertension suggests an early structural abnormality. Hypertension. 1999;34(4 Pt 1):655-658.

113. Baumbach GL, Heistad DD. Remodeling of cerebral arterioles in chronic hypertension. Hypertension. 1989;13(6 Pt 2):968-972.

114. Dunn WR, Wallis SJ, Gardiner SM. Remodelling and enhanced myogenic tone in cerebral resistance arteries isolated from genetically hypertensive Brattleboro rats. J Vasc Res. 1998;35(1):18-26.

115. Baumbach GL, Dobrin PB, Hart MN, Heistad DD. Mechanics of cerebral arterioles in hypertensive rats. Circ Res. 1988;62(1):56-64.

116. Sokolova IA, Manukhina EB, Blinkov SM, Koshelev VB, Pinelis VG, Rodionov IM. Rarefication of the arterioles and capillary network in the brain of rats with different forms of hypertension. Microvasc Res. 1985;30(1):1-9.

117. Jumar A, Harazny JM, Ott C, Kistner I, Friedrich S, Schmieder RE. Improvement in Retinal Capillary Rarefaction After Valsartan Treatment in Hypertensive Patients. J Clin Hypertens (Greenwich). 2016;18(11):1112-1118.

118. Sun C, Ladores C, Hong J, Nguyen DQ, Chua J, Ting D, Schmetterer L, Wong TY, Cheng CY, Tan ACS. Systemic hypertension associated retinal microvascular changes can be detected with optical coherence tomography angiography. Sci Rep. 2020;10(1):9580.

119. Chua J, Chin CWL, Hong J, Chee ML, Le TT, Ting DSW, Wong TY, Schmetterer L. Impact of hypertension on retinal capillary microvasculature using optical coherence tomographic angiography. J Hypertens. 2019;37(3):572-580.

120. Sedaghat S, Vernooij MW, Loehrer E, Mattace-Raso FU, Hofman A, van der Lugt A, Franco OH, Dehghan A, Ikram MA. Kidney Function and Cerebral Blood Flow: The Rotterdam Study. J Am Soc Nephrol. 2016;27(3):715-721.

121. Ikram MA, Vernooij MW, Hofman A, Niessen WJ, van der Lugt A, Breteler MM. Kidney function is related to cerebral small vessel disease. Stroke. 2008;39(1):55-61.

122. Zhuang X, Cao D, Zeng Y, Yang D, Yao J, Kuang J, Xie J, He M, Cai D, Zhang S, Wang W, Zhang L. Associations between retinal microvasculature/microstructure and renal function in type 2 diabetes patients with early chronic kidney disease. Diabetes Res Clin Pract. 2020;168:108373.

123. Mohandas R, Segal M, Srinivas TR, Johnson BD, Wen X, Handberg EM, Petersen JW, Sopko G, Merz CN, Pepine CJ. Mild renal dysfunction and long-term adverse outcomes in women with chest pain: results from the National Heart, Lung, and Blood Institute-sponsored Women's Ischemia Syndrome Evaluation (WISE). Am Heart J. 2015;169(3):412-418.

124. Mohandas R, Segal MS, Huo T, Handberg EM, Petersen JW, Johnson BD, Sopko G, Bairey Merz CN, Pepine CJ. Renal function and coronary microvascular dysfunction in women with symptoms/signs of ischemia. PLoS One. 2015;10(5):e0125374.
125. Sakamoto N, Iwaya S, Owada T, Nakamura Y, Yamauchi H, Hoshino Y, Mizukami H, Sugimoto K, Yamaki T, Kunii H, Nakazato K, Suzuki H, Saitoh S, Takeishi Y. A reduction of coronary flow reserve is associated with chronic kidney disease and long-term cardio-cerebrovascular events in patients with non-obstructive coronary artery disease and vasospasm. Fukushima J Med Sci. 2012;58(2):136-143.
126. Charytan DM, Skali H, Shah NR, Veeranna V, Cheezum MK, Taqueti VR, Kato T, Bibbo CR, Hainer J, Dorbala S, Blankstein R, Di Carli MF. Coronary flow reserve is predictive of the risk of cardiovascular death regardless of chronic kidney disease stage. Kidney Int. 2018;93(2):501-509.
127. Castro P, Azevedo E, Rocha I, Sorond F, Serrador JM. Chronic kidney disease and poor outcomes in ischemic stroke: is impaired cerebral autoregulation the missing link? BMC Neurol. 2018;18(1):21.
128. Prommer HU, Maurer J, von Websky K, Freise C, Sommer K, Nasser H, Samapati R, Reglin B, Guimarães P, Pries AR, Querfeld U. Chronic kidney disease induces a systemic microangiopathy, tissue hypoxia and dysfunctional angiogenesis. Sci Rep. 2018;8(1):5317.
129. Balk EM, Karas RH, Jordan HS, Kupelnick B, Chew P, Lau J. Effects of statins on vascular structure and function: a systematic review. Am J Med. 2004;117(10):775-790.
130. Ludwig S, Shen GX. Statins for diabetic cardiovascular complications. Curr Vasc Pharmacol. 2006;4(3):245-251.
131. Kohno M, Murakawa K, Yasunari K, Yokokawa K, Horio T, Kano H, Minami M, Yoshikawa J. Improvement of erythrocyte deformability by cholesterol-lowering therapy with pravastatin in hypercholesterolemic patients. Metabolism. 1997;46(3):287-291.
132. Tur E, Politi Y, Rubinstein A. Cutaneous blood flow abnormalities in hypertriglyceridemia. J Invest Dermatol. 1994;103(4):597-600.
133. Yamada M, Huang Z, Dalkara T, Endres M, Laufs U, Waeber C, Huang PL, Liao JK, Moskowitz MA. Endothelial nitric oxide synthase-dependent cerebral blood flow

augmentation by L-arginine after chronic statin treatment. J Cereb Blood Flow Metab. 2000;20(4):709-717.

134. Amin-Hanjani S, Stagliano NE, Yamada M, Huang PL, Liao JK, Moskowitz MA. Mevastatin, an HMG-CoA reductase inhibitor, reduces stroke damage and upregulates endothelial nitric oxide synthase in mice. Stroke. 2001;32(4):980-986.

135. Asahi M, Huang Z, Thomas S, Yoshimura S, Sumii T, Mori T, Qiu J, Amin-Hanjani S, Huang PL, Liao JK, Lo EH, Moskowitz MA. Protective effects of statins involving both eNOS and tPA in focal cerebral ischemia. J Cereb Blood Flow Metab. 2005;25(6):722-729.

136. Xu G, Fitzgerald ME, Wen Z, Fain SB, Alsop DC, Carroll T, Ries ML, Rowley HA, Sager MA, Asthana S, Johnson SC, Carlsson CM. Atorvastatin therapy is associated with greater and faster cerebral hemodynamic response. Brain Imaging Behav. 2008;2(2):94.

137. Forteza A, Romano JG, Campo-Bustillo I, Campo N, Haussen DC, Gutierrez J, Koch S. High-dose atorvastatin enhances impaired cerebral vasomotor reactivity. J Stroke Cerebrovasc Dis. 2012;21(6):487-492.

138. Freitas F, Estato V, Reis P, Castro-Faria-Neto HC, Carvalho V, Torres R, Lessa MA, Tibirica E. Acute simvastatin treatment restores cerebral functional capillary density and attenuates angiotensin II-induced microcirculatory changes in a model of primary hypertension. Microcirculation. 2017;24(8).

139. Haak E, Abletshauser C, Weber S, Goedicke C, Martin N, Hermanns N, Lackner K, Kusterer K, Usadel KH, Haak T. Fluvastatin therapy improves microcirculation in patients with hyperlipidaemia. Atherosclerosis. 2001;155(2):395-401.

140. Havelius U, Bergqvist D, Falke P, Hindfelt B, Krakau T. I. Impaired dark adaptation in symptomatic carotid artery disease. Neurology. 1997;49(5):1353-1359.

141. Kofoed PK, Munch IC, Holfort SK, Sillesen H, Jensen LP, Iversen HK, Larsen M. Cone pathway function in relation to asymmetric carotid artery stenosis: correlation to blood pressure. Acta Ophthalmol. 2013;91(8):728-732.

142. Sayin N, Kara N, Uzun F, Akturk IF. A quantitative evaluation of the posterior segment of the eye using spectral-domain optical coherence tomography in carotid artery stenosis: a pilot study. Ophthalmic Surg Lasers Imaging Retina. 2015;46(2):180-185.

143. Wang D, Li Y, Zhou Y, Jin C, Zhao Q, Wang A, Wu S, Wei WB, Zhao X, Jonas JB. Asymptomatic carotid artery stenosis and retinal nerve fiber layer thickness. A community-based, observational study. PLoS One. 2017;12(5):e0177277.

144. Çakır A, Düzgün E, Demir S, Çakır Y, Ünal MH. Spectral Domain Optical Coherence Tomography Findings in Carotid Artery Disease. Turk J Ophthalmol. 2017;47(6):326-330.

145. Heßler H, Zimmermann H, Oberwahrenbrock T, Kadas EM, Mikolajczak J, Brandt AU, Kauert A, Paul F, Schreiber SJ. No Evidence for Retinal Damage Evolving from Reduced Retinal Blood Flow in Carotid Artery Disease. Biomed Res Int. 2015;2015:604028.

146. Ali FS, Bader N, Zuberi BF, Banu S. Frequency of silent carotid artery stenosis in diabetics and its associated factors: An analysis in tertiary care hospital. Pak J Med Sci. 2020;36(6):1270-1274.

147. Hoke M, Schillinger M, Minar E, Goliasch G, Binder CJ, Mayer FJ. Carotid ultrasound investigation as a prognostic tool for patients with diabetes mellitus. Cardiovasc Diabetol. 2019;18(1):90.

148. Ratanakorn D, Kongsakorn N, Keandoungchun J, Tegeler CH. Prevalence and predictors of carotid stenosis in Thai patients with ocular disorders. J Clin Neurosci. 2013;20(6):862-866.

149. Marmion VJ, Aldoori MI, Woodcock JP, Stephenson J. A cohort study of duplex Doppler examinations of the carotid artery in primary open angle glaucoma. JRSM Open. 2014;5(8):2054270414527933.

150. Chou CC, Hsu MY, Lin CH, Lin CC, Wang CY, Shen YC, Wang IJ. Risk of developing open-angle glaucoma in patients with carotid artery stenosis: A nationwide cohort study. PLoS One. 2018;13(4):e0194533.

151. Kamtchum-Tatuene J, Noubiap JJ, Wilman AH, Saqqur M, Shuaib A, Jickling GC. Prevalence of High-risk Plaques and Risk of Stroke in Patients With Asymptomatic Carotid Stenosis: A Meta-analysis. JAMA Neurol. 2020;77(12):1524-1535.

152. Gupta A, Chazen JL, Hartman M, Delgado D, Anumula N, Shao H, Mazumdar M, Segal AZ, Kamel H, Leifer D, Sanelli PC. Cerebrovascular reserve and stroke risk in patients with carotid stenosis or occlusion: a systematic review and meta-analysis. Stroke. 2012;43(11):2884-2891.

153. Lahme L, Marchiori E, Panuccio G, Nelis P, Schubert F, Mihailovic N, Torsello G, Eter N, Alnawaiseh M. Changes in retinal flow density measured by optical coherence tomography angiography in patients with carotid artery stenosis after carotid endarterectomy. Sci Rep. 2018;8(1):17161.

154. Lee CW, Cheng HC, Chang FC, Wang AG. Optical Coherence Tomography Angiography Evaluation of Retinal Microvasculature Before and After Carotid Angioplasty and Stenting. Sci Rep. 2019;9(1):14755.

155. Araki CT, Babikian VL, Cantelmo NL, Johnson WC. Cerebrovascular hemodynamic changes associated with carotid endarterectomy. J Vasc Surg. 1991;13(6):854-859; discussion 9-60.

156. Yan J, Yang X, Wu J, Liu B, Jiao X, Li W, Guo M. Visual Outcome of Carotid Endarterectomy in Patients with Carotid Artery Stenosis. Ann Vasc Surg. 2019;58:347-356.

157. Guclu O, Guclu H, Huseyin S, Korkmaz S, Yuksel V, Canbaz S, Pelitli Gurlu V. Retinal ganglion cell complex and peripapillary retinal nerve fiber layer thicknesses following carotid endarterectomy. Int Ophthalmol. 2019;39(7):1523-1531.

158. Akca Bayar S, Kayaarası Öztürker Z, Pınarcı EY, Ercan ZE, Akay HT, Yılmaz G. Structural Analysis of the Retina and Choroid before and after Carotid Artery Surgery. Curr Eye Res. 2020;45(4):496-503.

159. De Caro J, Ciacciarelli A, Tessitore A, Buonomo O, Calzoni A, Francalanza I, Dell'Aera C, Cosenza D, Currò CT, Granata F, Vinci SL, Trimarchi G, Toscano A, Musolino RF, La Spina P. Variants of the circle of Willis in ischemic stroke patients. J Neurol. 2021;268(10):3799-3807.

160. Zaninovich OA, Ramey WL, Walter CM, Dumont TM. Completion of the Circle of Willis Varies by Gender, Age, and Indication for Computed Tomography Angiography. World Neurosurg. 2017;106:953-963.

161. Hoksbergen AW, Fülesdi B, Legemate DA, Csiba L. Collateral configuration of the circle of Willis: transcranial color-coded duplex ultrasonography and comparison with postmortem anatomy. Stroke. 2000;31(6):1346-1351.

162. North American Symptomatic Carotid Endarterectomy Trial. Methods, patient characteristics, and progress. Stroke. 1991;22(6):711-720.

163. Kluytmans M, van der Grond J, van Everdingen KJ, Klijn CJ, Kappelle LJ, Viergever MA. Cerebral hemodynamics in relation to patterns of collateral flow. Stroke. 1999;30(7):1432-1439.

164. Sundt TM, Sharbrough FW, Anderson RE, Michenfelder JD. Cerebral blood flow measurements and electroencephalograms during carotid endarterectomy. J Neurosurg. 1974;41(3):310-320.

165. Kaszczewski P, Elwertowski M, Leszczyński J, Ostrowski T, Kaszczewska J, Gałązka Z. Intracranial Flow Volume Estimation in Patients with Internal Carotid Artery Occlusion. Diagnostics (Basel). 2022;12(3).

166. Liebeskind DS. Collateral circulation. Stroke. 2003;34(9):2279-2284.

167. Zarrinkoob L, Wåhlin A, Ambarki K, Birgander R, Eklund A, Malm J. Blood Flow Lateralization and Collateral Compensatory Mechanisms in Patients With Carotid Artery Stenosis. Stroke. 2019;50(5):1081-1088.

168. Yamamoto H, Schmidt-Kastner R, Hamasaki DI, Parel JM. Complex neurodegeneration in retina following moderate ischemia induced by bilateral common carotid artery occlusion in Wistar rats. Exp Eye Res. 2006;82(5):767-779.

169. Lee D, Kang H, Yoon KY, Chang YY, Song HB. A mouse model of retinal hypoperfusion injury induced by unilateral common carotid artery occlusion. Exp Eye Res. 2020;201:108275.

170. Orihashi K, Matsuura Y, Sueda T, Shikata H, Morita S, Hirai S, Sueshiro M, Okada K. Flow velocity of central retinal artery and retrobulbar vessels during cardiovascular operations. J Thorac Cardiovasc Surg. 1997;114(6):1081-1087.

9. Bibliography of the candidate's publications

9.1 Publications related to the PhD thesis

1. **István L**, Czakó C, Benyó F, Élő Á, Mihály Z, Sótonyi P, Varga A, Nagy ZZ, Kovács I. The effect of systemic factors on retinal blood flow in patients with carotid stenosis: an optical coherence tomography angiography study. GEROSCIENCE: OFFICIAL JOURNAL OF THE AMERICAN AGING ASSOCIATION (AGE) 44: 1 pp. 389-401. (2022) **IF: 5,6**

2. **István L**, Czakó C, Élő Á, Mihály Z, Sótonyi P, Varga A, Ungvári Z, Csiszár A, Yabluchanskiy A, Conley S, Csipő T, Lipecz Á, Kovács I, Nagy ZZ. Imaging retinal microvascular manifestations of carotid artery disease in older adults: from diagnosis of ocular complications to understanding microvascular contributions to cognitive impairment. GEROSCIENCE: OFFICIAL JOURNAL OF THE AMERICAN AGING ASSOCIATION (AGE) 43: 4 pp. 1703-1723. (2021) **IF: 7,5811**

3. Mihály Z*, **István L***, Czakó C, Benyó F, Borzsák S, Varga A, Magyar-Stang R, Banga PV, Élő Á, Debreczeni R, Kovács I, Sótonyi P. The Effect of Circle of Willis Morphology on Retinal Blood Flow in Patients with Carotid Stenosis Measured by Optical Coherence Tomography Angiography. JOURNAL OF CLINICAL MEDICINE 12: 16 Paper: 5335, 13 p. (2023) **IF: 3,0**
   *co-first authorship

4. Czakó C, István L, Benyó F, Élő Á, Erdei G, Horváth H, Nagy ZZ, Kovács I. The Impact of Deterministic Signal Loss on OCT Angiography Measurements. TRANSLATIONAL VISION SCIENCE AND TECHNOLOGY 9: 5 Paper: 10, 9 p. (2020) **IF: 3,283**

Σ Impact factor:19,464

9.2. Publications not related to the PhD thesis

1. Lengyel B, Magyar-Stang R, Pál H, Debreczeni R, Sándor ÁD, Székely A, Gyürki D, Csippa B, **István L**, Kovács I, Sótonyi P, Mihály Z. Non-Invasive Tools in Perioperative Stroke Risk Assessment for Asymptomatic Carotid Artery Stenosis with a Focus on the Circle of Willis. JOURNAL OF CLINICAL MEDICINE 13: 9 Paper: 2487, 21 p. (2024) **IF: 3,0***
   * expected IF value

2. Benyó F, **István L**, Kiss H, Gyenes A, Erdei G, Juhász É, Vlasak N, Unger C, Andorfi T, Réz K, Kovács I, Nagy ZZ. Assessment of Visual Quality Improvement as a Result of Spectacle Personalization. LIFE-BASEL 13: 8 Paper: 1707, 16 p. (2023) **IF: 3,2**

3. Gyenes A, **István L**, Benyó F, Papp A, Resch M, Sándor N, Józsi M, Nagy ZZ, Kovács I, Kiss S. Intraocular neutralizing antibodies against aflibercept in patients with age related macular degeneration. **BMC OPHTHALMOLOGY 2**3: 1 Paper: 14, 8 p. (2023) **IF: 1,7**

4. **István L**, Nagy ZZ, Kovács I. Parafoveal capillary density as a potential biomarker in the assessment of diabetic retinopathy progression. DEVELOPMENTS IN HEALTH SCIENCES 6: 1 pp. 17-21. (2023)

5. Magyar-Stang R, **István L**, Pál H, Csányi B, Gaál A, Mihály Z, Czinege Z, Sótonyi P, Horváth T, Koller Á, Bereczki D, Kovács I, Debreczeni R. Impaired cerebrovascular reactivity correlates with reduced retinal vessel density in patients with carotid artery stenosis: Cross-sectional, single center study. PLOS ONE 18: 9 Paper: e0291521, 18 p. (2023) **IF: 2,9**

6. Fehér J, Élő Á, **István L**, Nagy ZZ, Radák Z, Scuderi G, Artico M, Kovács I. Microbiota mitochondria disorders as hubs for early age-related macular

degeneration. GEROSCIENCE: OFFICIAL JOURNAL OF THE AMERICAN AGING ASSOCIATION (AGE) 44: 6 pp. 2623-2653. (2022) **IF: 5,6**

7. **István L**, Czakó C, Gyenes A, Nagy ZZ, Kovács I. A carotis-szűkület hatása a retina érhálózatának sűrűségére OCT-angioigráfiás vizsgálatok során [The effect of carotid artery stenosis on retinal microcirculation with optical coherence tomography angiography] SZEMÉSZET 159: 4 pp. 174-177. (2022)

8. **István L**, Benyó F, Csorba A, Jimoh IJ, Gál A, Molnár MJ, Nagy ZZ, Szabó V. Cornealis polymegathismus és retinalis pigmenthám-eltérések MELAS-szindrómában [Corneal polymegathism and pigmentary retinopathy in MELAS syndrome – a case report] SZEMÉSZET 159: 2 pp. 69-75. (2022)

9. Végh A, Csorba A, Koller Á, Mohammadpour B, Killik P, **István L**, Magyar M, Fenesi T, Nagy ZZ. Presence of SARS-CoV-2 on the conjunctival mucosa in patients hospitalized due to COVID-19: Pathophysiological considerations and therapeutic implications. PHYSIOLOGY INTERNATIONAL 109: 4 pp. 475-485. (2022) **IF: 1,4**

10. Nagy ZZ, Dormán P, Csorba A, Kovács K, Benyó F, **István L**, Kiss H. A hályogsebészet helyzete Magyarországon 2020-ban a "Katarakta regiszter" eredményeinek összegzése. SZEMÉSZET 158: 3 pp. 138-143. (2021)

11. Czakó C, Kovács T, Ungvári Z, Csiszar A, Yabluchanskiy A, Conley S, Csipő T, Lipécz Á, Horváth H, Sándor GL, **István L**, Trevor L, Nagy ZZ, Kovács I. Retinal biomarkers for Alzheimer's disease and vascular cognitive impairment and dementia (VCID): implication for early diagnosis and prognosis. GEROSCIENCE: OFFICIAL JOURNAL OF THE AMERICAN AGING ASSOCIATION (AGE) 42: 6 pp. 1499-1525. (2020) **IF: 7,713**

12. Élő Á, Czakó C, **István L**, Benyó F, Nagy ZZ, Kovács I. Retinalis biomarkerek szerepe a vascularis dementia és az Alzheimer-kór korai formáinak

diagnosztikájában [Retinal biomarkers for early diagnosis of vascular dementia and Alzheimer's disease]. ORVOSI HETILAP 161: 41 pp. 1744-1752. (2020) **IF: 0,540**

13. Mihály Z, Fontanini DM, Sándor ÁD, Dósa E, Lovas G, Kolossváry E, Kovács I, **István L**, Entz L, Sótonyi P. A nyaki verőér-szűkületes betegek ellátási irányelveinek különbségei Európa különböző országaiban [Differences in guidelines for patients with carotid artery stenosis in some European countries]. ORVOSI HETILAP 161: 51 pp. 2139-2145. (2020) **IF: 0,540**

14. Czakó C, **István L**, Ecsedy M, Récsán Z, Sándor G, Benyó F, Horváth H, Papp A, Resch M, Borbándy Á, Nagy ZZ, Kovács I. The effect of image quality on the reliability of OCT angiography measurements in patients with diabetes. INTERNATIONAL JOURNAL OF RETINA AND VITREOUS 5: 1 Paper: 46, 7 p. (2019)

10. Acknowledgements

First and foremost, I would like to thank my supervisor, Illés Kovács, for his vote of confidence in me to join the working group. I am grateful for his guidance and support throughout my work both in terms of research and clinical practice.

I would like to thank Professor **Zoltán Zsolt Nagy** for giving me the opportunity to conduct my research at the Department of Ophthalmology and for his support in my professional development.

I would like to thank Professor **Péter Sótonyi, Zsuzsa Mihály,** and their colleagues at the Department of Vascular Surgery for the smooth running of this large-scale study; it was a pleasure to work with such enthusiastic and professional colleagues.

I am grateful to **Zsuzsa Récsán** for her trust and professional support since the beginning of my career.

I want to thank **Mónika Ecsedy**, **Béla Csákány,** and **Miklós Resch** for their continuous help.

Special thanks go to **Cecilia Czakó** for always helping me when I was lost in the maze of research work and to **Anita Csorba** for sharing her experience in writing a PhD thesis, and for her constant encouragement in completing my work.

I would also like to thank my colleagues, **Fruzsina Benyó**, **Andrea Gyenes**, **Dorottya Kriskó,** and **Judit Rynkiewicz**, who have become true friends over the years and are always there for me. I would also like to thank all my colleagues for sharing their professional knowledge; I consider myself lucky to learn from the best professionals. I would especially like to express my gratitude for the support of my colleagues during my recovery; every message of encouragement has given me unspeakable strength to overcome the difficulties.

Last but not least, I would like to express my heartfelt gratitude to my family for their continued support. Without their constant encouragement, this work would not have been accomplished.